

12

A. AD-A172 274

# Soviet Research on the Transport of Intense Relativistic Electron Beams Through Low-Pressure Air

Nikita Wells

DTIC FILE COPY

This document has been approved  
for public release and sale; its  
distribution is unlimited.

A  
DTIC  
ELECTE  
SEP 23 1986  
S D E

**Rand**

86 9 23 070

The research described in this report was sponsored by the Defense Advanced Research Projects Agency under a Federally Funded Research and Development Center relationship with the Office of the Secretary of Defense under Contract No. MDA903-85-C-0030.

**Library of Congress Cataloging in Publication Data**

Wells, Nikita, 1937-

Soviet research on the transport of intense relativistic electron beams through low-pressure air.

"August 1986."

"R-3309-ARPA."

Bibliography: p.

1. Electron beams. 2. Plasma (Ionized gases)  
3. Electron beams—Research—Soviet Union. I. United States. Defense Advanced Research Projects Agency.  
II. Rand Corporation. III. Title.  
QC793.5.E622W44 1986 539.7'2112 86-10008  
ISBN 0-8330-0718-1

**The Rand Publication Series:** The Report is the principal publication documenting and transmitting Rand's major research findings and final research results. The Rand Note reports other outputs of sponsored research for general distribution. Publications of The Rand Corporation do not necessarily reflect the opinions or policies of the sponsors of Rand research.

**Published by The Rand Corporation**

SECURITY CLASSIFICATION OF THIS PAGE (When Data Entered)

# REPORT DOCUMENTATION PAGE

READ INSTRUCTIONS  
BEFORE COMPLETING FORM  
RECIPIENT'S CATALOG NUMBER

1. REPORT NUMBER R-3309-ARPA		2. GOVT ACCESSION NO. <del>111111</del>	
4. TITLE (and Subtitle) Soviet Research on the Transport of Intense Relativistic Electron Beams Through Low- Pressure Air		3. TYPE OF REPORT & PERIOD COVERED Interim	
7. AUTHOR(s) Nikita Wells		6. PERFORMING ORG. REPORT NUMBER	
9. PERFORMING ORGANIZATION NAME AND ADDRESS The Rand Corporation 1700 Main Street Santa Monica, CA 90406		8. CONTRACT OR GRANT NUMBER(s) MDA903-85-C-0030	
11. CONTROLLING OFFICE NAME AND ADDRESS Defense Advanced Research Projects Agency Department of Defense Arlington, VA 22209		10. PROGRAM ELEMENT, PROJECT, TASK AREA & WORK UNIT NUMBERS	
14. MONITORING AGENCY NAME & ADDRESS (if different from Controlling Office)		12. REPORT DATE August 1986	
		13. NUMBER OF PAGES 51	
		15. SECURITY CLASS. (of this report) Unclassified	
		15a. DECLASSIFICATION/DOWNGRADING SCHEDULE	
16. DISTRIBUTION STATEMENT (of this Report) Approved for Public Release - Distribution Unlimited			
17. DISTRIBUTION STATEMENT (of the abstract entered in Block 20, if different from Report) No Restrictions			
18. SUPPLEMENTARY NOTES			
19. KEY WORDS (Continue on reverse side if necessary and identify by block number) Electron Beams USSR			
20. ABSTRACT (Continue on reverse side if necessary and identify by block number) see reverse side			

DD FORM 1 JAN 73 1473

SECURITY CLASSIFICATION OF THIS PAGE (When Data Entered)

This report analyzes Soviet research on the transport of intense relativistic electron beams (IREB) through low-pressure air and other gases without external magnetic fields. It reviews research reported in open-source technical publications from seven Soviet research institutes. These research papers indicate that Soviet interest in long-distance IREB transport at low gas pressure has endured from 1979 to the present.



R-3309-ARPA

Accession For	
NTIS GRA&I	<input checked="" type="checkbox"/>
DTIC TAB	<input type="checkbox"/>
Unannounced	<input type="checkbox"/>
Justification	
By	
Distribution/	
Availability Codes	
Dist	Avail and/or Special
A-1	

# **Soviet Research on the Transport of Intense Relativistic Electron Beams Through Low-Pressure Air**

Nikita Wells

August 1986

Prepared for the  
Defense Advanced Research  
Projects Agency

## PREFACE

This report was prepared in the course of a continuing Rand study of Soviet research and development of high-current, high-energy, charged particle beams and their scientific and technological applications. The work was sponsored by the Defense Advanced Research Projects Agency, Office of the Secretary of Defense (OSD), under Rand's OSD-supported Federally Funded Research and Development Center. It was carried out for the National Security Research Division in the Applied Science and Technology Program.

The report examines recent Soviet research on the propagation of intense relativistic electron beams through low-pressure air and gases, ( $10^{-6}$  Torr  $< P < 10^{-3}$  Torr), as reported in Soviet open-source technical publications. A follow-on report will discuss Soviet research on the propagation of intense relativistic electron beams through higher-pressure air and gases ( $P > 10^{-2}$  Torr).

The present report should be of interest to specialists in pulsed-power and high-current, charged particle beam research.

## SUMMARY

Soviet research on the propagation of intense relativistic electron beams (IREB) through air and gases has demonstrated the existence of several pressure ranges for possible efficient IREB propagation. The Soviets have recently paid specific attention to the low-pressure range from  $10^{-6}$  to  $10^{-3}$  Torr. Based on Soviet open-source technical literature published over the past fifteen years, the present report analyzes Soviet research on IREB propagation through this low-pressure range for air and other gases. IREB propagation in the pressure range from  $10^{-2}$  Torr to atmospheric will be considered in a follow-on Rand report.

The Soviet research has been carried out by at least seven research institutes from the end of the 1970s to the present, with most of it centered at the All-Union Electrical Engineering Institute (VEI) in Moscow. A significant part of the research concerns IREB propagation through the ionosphere and is performed by the Leningrad State University (LGU).

Soviet theoretical analysis concentrated on the formation of a quasi-equilibrium beam and the derivation of an expression for its propagation through low-pressure gas, taking into account space-charge forces, self-focusing of the beam, and the effect of the beam's own magnetic field on its focusing properties. The analysis involved the determination of equilibrium-beam formation time, relaxation length, density distribution of plasma formed by the passage of the beam, and the effects of beam parameters upon this background plasma.

Experimental investigation of the quasi-equilibrium beam demonstrated that it has a Bennett profile, determined the beam formation time, and showed that formation time decreases with increasing pressure and propagation length. For a 300 keV, 100 A beam, transverse beam temperature was found to be 0.5 keV near the beam focus, and 2 keV downstream of the focus. No dependence of beam front velocity upon propagation length had been observed.

The high transverse beam temperature was attributed to collective processes involved in beam interaction with background gas. The high temperature was, in turn, thought to cause the observed low-frequency oscillations of beam current density. The amplitude of these oscillations was found to increase in the direction of beam propagation; the rate of increase was determined by the concentration of beam-produced plasma. Soviet researchers concluded that the beam spreads by scattering produced by the field of the transversely oscillating gas ions.

The final conclusion was that beam-spreading can be prevented by controlling plasma density.

A significant research project has been under way at LGU, where Soviet researchers have been studying IREB transport at high altitudes, taking into account the effect of polarized ionospheric plasma, the electron concentration, and the earth's magnetic field at various altitudes for both day and night atmospheres. LGU calculated that an IREB can propagate with beam currents greater than 1 MA for electron beam energies greater than 22 MeV, in the area of maximum electron concentration in the ionosphere. LGU also demonstrated that when the IREB is injected parallel to the earth's magnetic field, the magnetic field can play an important part in stabilizing the beam when the electron concentration drops (as during the night). The maximum beam current density was shown to depend only upon the local maximum value of electron concentration. The limit of beam propagation distance has been determined to be from 1.5 km to 11 km, depending upon pitch angle of injection and geomagnetic latitude for a 2 MeV, 1 meter radius beam at a 300 km altitude.

Four Soviet research institutes have independently demonstrated that the use of an insulated channel increases IREB transport dramatically. This conclusion was based on measurements of the energy and current of ions trapped in the IREB, the beam pulse delay time, erosion of the beam pulse leading front, and the dependence of channel length upon beam divergence; IREB propagation was found to be independent of the insulator material.

The Soviet emphasis on effective IREB propagation through low-pressure air may be significant. The low-pressure range coincides with that encountered in the upper atmosphere and therefore may relate to tests and long-distance IREB transport analysis for military and space applications.



## ACKNOWLEDGMENTS

The author would like to thank Martin Lampe of the Naval Research Laboratory and Han S. Uhm of the Naval Surface Weapons Center for their reviews of this report and for their many useful suggestions. He is also grateful to his colleagues at The Rand Corporation: Robert W. Salter and Cullen M. Crain for reviewing the report; Simon Kassel for direction, support of, and interest in the project; and Nathan Brooks for assistance in accumulating and organizing the Soviet technical data.

Scripta Technica, Inc., a subsidiary of John Wiley & Sons, Inc., publishers, kindly granted permission to reproduce graphics taken from the Soviet scientific journal *Radio Engineering and Electronic Physics* (*Radiotekhnika i elektronika*), appearing herein as Figs. 1-12.

The American Institute of Physics kindly granted permission to reproduce graphics taken from three Soviet scientific journals: *Soviet Technical Physics Letters* (*Pis'ma v zhurnal tekhnicheskoy fiziki*), graphics appearing herein as Figs. 13, 16, and 17; *Soviet Technical Physics* (*Zhurnal tekhnicheskoy fiziki*), graphics appearing herein as Figs. 14, 15, and 26-36; and *Soviet Journal of Plasma Physics* (*Fizika plazmy*), graphics appearing herein as Figs. 18-25.

## CONTENTS

PREFACE .....	iii
SUMMARY .....	v
ACKNOWLEDGMENTS .....	vii
FIGURES .....	xi
TABLES .....	xiii
Section	
I. INTRODUCTION .....	1
II. IREB PROPAGATION THROUGH RAREFIED GAS .....	3
VEI Research .....	3
IYaF-TPI Experiments .....	17
LGU Ionospheric Models .....	22
IFAN Low Current Experiments .....	25
III. IREB PROPAGATION EXPERIMENTS UTILIZING INSULATED CHANNELS .....	26
FIAN Research .....	26
YeGU Research .....	35
OIYaI Research .....	40
IV. CONCLUSIONS .....	45
REFERENCES .....	47

## FIGURES

1. Change in the Phase Diagram of a Cold Electron Beam in a Collisionless Relaxation Process . . . . .	4
2. Electron Trajectories in the Proximity of the First Focus . .	5
3. Beam Envelope $r_{0.5}$ Determining the Relation $I(r_{0.5})/I_b = 0.5$ as a Function of $z$ for $i = 0.034$ and $i = 0.0034$ . . . . .	5
4. Current Density Radial Distribution. . . . .	6
5. Comparison of the $j(\rho)$ Distribution Normalized to the Initial Current Density $j_0 = I_b/\pi a_g^2$ with the Initial Characteristic Radius $a_g$ (Curve 1) to the Dependence Obtained by the Numerical Calculations (Curve 2) . . . . .	7
6. Average Beam Structure as a Function of Propagation Length. . . . .	10
7. Oscilloscope Trace of the Beam Current on the (1) Central and (2) Outer Collector Plates. . . . .	11
8. Dependence of the Average Oscillation Frequency as a Function of Pressure for Different Beam Currents: Curve (1), $I_b = 50$ to $70$ A; Curve (2), $I_b = 30$ to $50$ A . . . . .	11
9. Relative Oscillation Amplitude as a Function of Length Along the Beam for Several Different Pressures. . . . .	12
10. Dependence of the Inverse of the Formation Time ( $t_1$ ) of Oscillations as a Function Beam Propagation Length for Different Pressures . . . . .	13
11. Oscillograms Showing the REB Propagation through Background Gas . . . . .	15
12. Velocities of the Electron Beam Propagation as a Function of Background Gas Pressure . . . . .	16
13. Electron Beam Transport Experimental Apparatus. . . . .	18
14. Beam Current Delay Time Measured at the Faraday Cup ( $L = 32$ cm) as a Function of Background Pressure . . . . .	19
15. $I_b/I_D$ Ratio as a Function of Background Pressure . . . . .	20
16. Dependence of Beam Current (at the Output of the Drift Tube) as a Function of Plasma Density . . . . .	21
17. Beam Propagation through the Insulated Wall Channel as a Function of Channel Length. . . . .	27
18. Schematic of the Experimental Apparatus. . . . .	28
19. The Effective Beam Transport Efficiency $I_{out}/I_{in}$ and the Output Beam Current Delay ( $\tau$ ) as a Function of Channel Length . . . . .	29

20.	The IREB Equilibrium Diameter Formation in an Insulated Channel of Length L. Beam Injection Voltage 500 kV, Beam Current 5 kA . . . . .	30
21.	IREB Equilibrium Diameter as a Function of Beam Current for Beam Transport through an Insulated Channel. . . . .	31
22.	The Effective Beam Transport Efficiency $I_{out}/I_{in}$ through a 20 cm Long Insulated Channel for Different Ratios of the Equilibrium Diameter to Cathode Diameter . . . . .	31
23.	Beam Current Pulse Injected into the Channel (Top Curve) and at the Output of the Channel (18 cm Long and 3.4 cm in Diameter). . . . .	32
24.	Ion Current Pulses on Collectors Located 75 cm (Top) and 100 cm (Bottom) after the Insulated Channel; the Calibration Frequency Used is 100 MHz. . . . .	33
25.	Effective Beam Transport Efficiency as a Function Time for a Conical Insulated Channel. . . . .	34
26.	Dependence of the IREB Dispersion Angle Upon the Transport Length Within an Insulated Channel of 4.2 cm Diameter . . . . .	36
27.	Dependence of the Beam Radius (Curves 1-3) and Beam Current Density Along the Beam Axis (Curves 4-6) as a Function of Distance Along the Channel. Copper Channel of 80 mm Length (1, 4) and Insulated Channels of 80 mm Length (2, 5) and 40 mm Length (3, 6). . . . .	36
28.	IREB Current Density Distribution Along the Beam Cross-Section at the Output of the Transport Channel . . . .	37
29.	Schematic of the Experimental Apparatus. . . . .	39
30.	Dependence of Transport Efficiency ( $I_{tr}/I_0$ ) Upon Background Air Pressure for Different Transport Channels. . . .	39
31.	Schematic Diagram of Experimental Apparatus . . . . .	41
32.	Dependence of the Electric Field Between the Grid Electrode and Insulated Channel Wall Upon the Channel Pressure . . . . .	42
33.	Dependence of the Electric Field Amplification Coefficient K Upon the Metal Grid Wire Diameter . . . . .	42
34.	Distribution of the Plasma Electron Concentration N as a Function of Time T. . . . .	43
35.	Distribution of the Plasma Electron Concentration N as a Function of Coordinates: Length, L; radius, R; and Azimuth, $\varphi$ . Energy in the Discharge Circuit Equal to 1,600 Joules . . . . .	44
36.	Dependence of the Plasma Electron Concentration Component N as a Function of the Background Gas P in a Polyvinyl Chloride Insulator Channel with Energy in the Discharge Circuit. . . . .	44

## TABLES

1.	Electron Concentration in the Upper Atmosphere . . . . .	23
2.	Parameters of an Equilibrium IREB for Plasma Electron Concentration $N = 3 \times 10^6 \text{ cm}^3$ . . . . .	24

## I. INTRODUCTION

This report analyzes Soviet research on the transport of intense relativistic electron beams (IREB) through low-pressure air and other gases (in the pressure range of  $10^{-3}$  to  $10^{-6}$  Torr) without external magnetic fields. In the absence of external magnetic fields, effective transport of such beams can be accomplished only by space-charge neutralization that is possible at pressures greater than  $10^{-6}$  Torr. Beam neutralization then takes place through gas ionization and the accumulation of positive ions within the electron beam. Another important factor is the electron beam's own magnetic field, which contributes to the compression (or self-focusing) of the beam in contrast to the beam's spreading due to electrostatic repulsion forces of the beam electrons.

These considerations were the basis of research performed by at least seven Soviet research institutes from the end of the 1970s to the present: All-Union Electrical Engineering Institute, Moscow (VEI); Nuclear Physics Research Institute of the Tomsk Polytechnical Institute (IYaF-TPI); Leningrad State University (LGU); Physics Institute, Kiev (IFAN); Lebedev Physics Institute, Moscow (FIAN); Physics of Condensed Matter Research Institute, Yerevan State University (YeGU); and Joint Institute of Nuclear Research, Dubna (OIIYaI). Most of this research has been performed by a team of at least 17 authors associated with VEI.

The VEI research team breaks down into three groups. Group A has published theoretical papers on long-distance IREB transport and IREB relaxation to an equilibrium beam state. At least seven papers were published on this subject from 1981 to 1984. One of these papers considers theoretically the propagation of a 2 kA, 10 GW (5 MeV) IREB for a distance of 1000 km. The paper concludes that the beam radius increase could be kept down to 10 percent. The optimum pressure for this case was determined to be  $8 \times 10^{-5}$  Torr.

Group B published five experimental papers on the transport of a 300 keV IREB through low-pressure air. The group stipulated a distance of 10 meters, beam currents of about 100 A, and 100  $\mu$ s pulse lengths. The experiments were made with 1975 equipment used by K. V. Khodatayev, one of the leading Soviet researchers on IREB propagation in air. Research was concentrated on transient processes of IREB transport, leading to the formation of a quasi-equilibrium IREB structure propagating in a path free from external magnetic fields.

Measurements were made of the IREB wavefront velocities, IREB energy spectra, lateral electron temperatures, low-frequency-beam current density oscillations formed after the first beam focus, and IREB dispersion velocities.

Group C published many theoretical papers on IREB transport in background gas with space-charge neutralization, radial IREB oscillations, return-current considerations, IREB's own B field compression, quasi-Bennett beam stability, etc.

The IYAF-TPI research is represented by four experimental papers on IREB transport of  $\mu\text{s}$  and ns pulsed beams through low-pressure gas, including space-charge neutralization and the beam's own magnetic field. The investigators have looked at the time necessary for the accumulation of ions by the beam by varying the background pressure and by using insulated wall beam-transport channels. Electron beams of 250 keV, 10 kA, 2  $\mu\text{s}$ , and 1.5 MeV, 30 kA, 50 ns have been used.

LGU research has published at least six papers dealing with theoretical analysis of IREB transport at high altitudes above the earth (100 km and above). These calculations took into account the beam's stabilization by the polarized ionospheric plasma, the ionosphere's electron concentration, and the earth's magnetic field for various altitudes for day and night atmospheres, and space-charge neutralization of the beam by plasma ions.

IFAN has published at least 10 experimental papers covering space-charge neutralization of electron beams transported through gas, self-focusing of neutralized IREB, the excitation of ion oscillations by the passage of IREB through gas, and the interaction of a density-modulated IREB with plasma, where nonlinear, quasi-equilibrium waves are formed. These experiments were performed with low-beam currents (up to 250 mA) and energies up to 20 keV in the background pressure range from  $10^{-5}$  to  $10^{-3}$  Torr.

The other three institutes produced a few papers on the use of insulated channels to help transport IREB at low pressures. OIYA I experimentally investigated IREB transport through a plasma channel set up inside an insulated metal pipe at a pressure of about  $10^{-5}$  Torr. The wall plasma inside the channel was reported to be very homogeneous, stable, and controllable in the pressure range from  $10^{-2}$  to  $10^{-5}$  Torr, independently of the electron beam being transported. FIAN and YeGU considered IREB transport through insulated channels and the effect of these channels upon the beam parameters. Beam transport even through bent channels has recently been shown to be possible.

The above research papers indicate an enduring (from 1979 to the present) Soviet interest in long-distance IREB transport at low gas pressure.

## II. IREB PROPAGATION THROUGH RAREFIED GAS

### VEI RESEARCH

#### VEI Theoretical Research

VEI theoretical analysis of IREB transport through low-pressure air and gases postulates quasi-equilibrium IREB and takes into account the beam's own magnetic field.

Criteria were established on the beam's magnetic limitations and the propagation length over which the beam can still be considered to have a quasi-Bennett distribution. Soviet researchers stressed the importance of the beam's self-fields for the transferring of energy at great distances. In 1981, VEI computed the optimum background pressure for a 10 GW, 2 kA electron beam propagating to a distance of 1000 km. Limitations on the divergence of the beam were imposed by allowing the beam radius to increase only by 10 percent over that distance. The avowed application for this calculation was stated to be the development of new means of energy transmission at great distances. The optimum background pressure was found to be  $P \approx 8 \times 10^{-5}$  Torr [1].

In the same year, VEI investigated the density distribution of plasma formed by an electron beam, with energies from 100 keV to 1 MeV and beam currents greater than 1 A, passing through an infinite transport pipe filled with neutral gas with pressures ranging from 1 to  $10^{-5}$  Torr. Plasma concentration as a function of beam current and gas pressure, and plasma density distribution as a function of beam radius, were determined theoretically. Individual regions of IREB transport have been mapped out as a function of beam current and gas density [2].

The collisionless relaxation of a cold electron beam was investigated theoretically and with numerical analysis at VEI in 1982 in Ref. 3. This beam relaxation means the transformation of the electron beam to a quasi-equilibrium state. It had been postulated by B. V. Chirikov et al. [4] back in 1971 that an IREB having an inhomogeneous density profile is a classic example of a medium made up of particles oscillating to a nonlinear dependence, having a wide spectrum of betatron oscillations, and that this medium as a result of intensive mixing strives asymptotically to obtain an equilibrium distribution.



In Ref. 3, VEI investigated a particle system with an inhomogeneous density profile and zero emittance. For this case the phase diagram at the initial time appears as a straight line. With passing time the line in the phase diagram takes on a wavy character and then turns it into a spiral due to the non-isochronism of the different particle betatron oscillations, as first shown by K. V. Khodatayev in 1973 in Ref. 5 and represented in Fig. 1. As a final result, the spiral fills the phase diagram completely while the diagram's area tends asymptotically to reach a constant value.

The study of the beam relaxation was made with the assumption of a cold, space-charge-neutralized beam having zero initial temperature, zero emittance, and cylindrical geometry. The initial electron velocity and angular distributions were neglected, and ions were considered to be nonmovable. It was assumed that at  $x = 0$  the electron space distribution has a Gaussian distribution with radius  $a_0 = a_g$  that was cut off at a radius of  $2a_g$ . The basic difference between a Bennett distribution and the case looked at in Ref. 3 is that the equilibrium Bennett distribution fulfills the condition of the local magnetohydrodynamic equilibrium between the forces of magnetic compression and temperature-spreading of the electron beam (as shown in Ref. 1), whereas in the case of Ref. 3 the equilibrium is obtained dynamically for each electron separately (as shown in Ref. 6).

The results of the calculations made in Ref. 3 are presented in Fig. 2, which shows the electron trajectories in the area of the first focus. Figure 3 shows the dependence of the beam envelope  $r_{0.5}$  determining the relation  $I(r_{0.5})/I_b = 0.5$  as a function of  $z$ . Figure 4 depicts the change in the radial distribution of the current density  $j(r)$  in the beam relaxation process into the equilibrium state.

It is seen that, after one well-defined focus, the beam relaxes to a quasi-equilibrium state that is characterized by a strong mixing of the

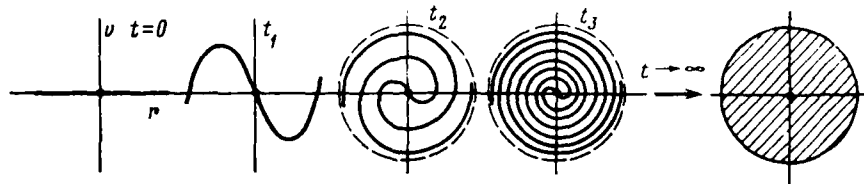


Fig. 1—Change in the phase diagram of a cold electron beam in a collisionless relaxation process [3]

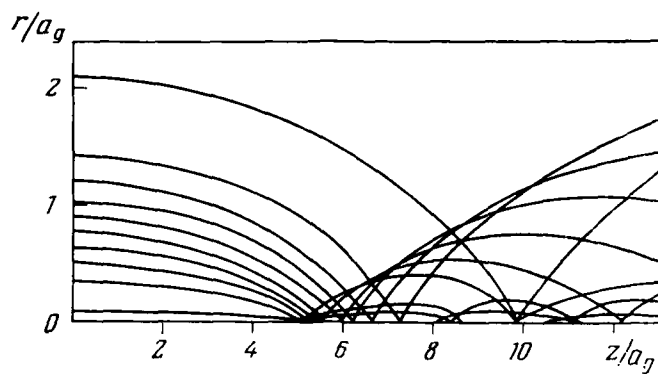


Fig. 2—Electron trajectories in the proximity of the first focus [3]

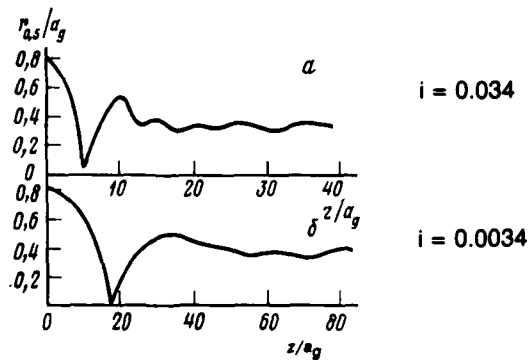


Fig. 3—Beam envelope  $r_{0.5}$  determining the relation  $I(r_{0.5})/I_b = 0.5$  as a function of  $z$  for  $i = 0.034$  and  $i = 0.0034$  [3]; ( $i$  is the layer number used in the numerical calculations)

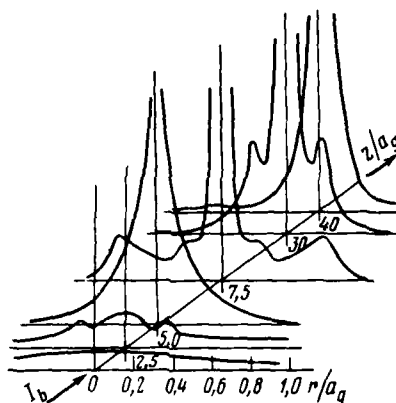


Fig. 4—Current density radial distribution [3]

beam trajectories, smooth distribution of the current density, and the characteristic transverse beam size of radius  $a \approx 0.4a_g$  (with  $a_g$  representing the Gaussian equilibrium radius). The relation of  $a/a_g$  does not depend upon the beam current but is determined only by the initial and final electron distribution.

The numerical calculations were made by breaking up the beam into 100 concentric layers, the movement of each of which was determined by Eq. (1), in cylindrical coordinates, as derived in Ref. 3 with initial conditions  $\rho_i = \rho_{i0}$ ,  $\rho'_i = 0$ , where  $i$  is the layer number.

$$\rho'' = -2i\varphi(\rho, x) \frac{(1 + \rho'^2)^{3/2}}{\rho} \quad (1)$$

where  $\rho = r/a_0$ ,  
 $x = z/a_0$ , and  
 $\varphi(\rho, x)$  = the value of beam current flowing inside the cylindrical contour (of radius  $\rho$ ) with a fixed  $x$ . (The value  $a_0$  does not enter the dimensionless Eq. (1), and this is why the calculations do not show a dependence upon current density.)

It is also seen (in Fig. 3) that  $a/a_g$  does not depend upon the layer number parameter  $i$  for a large change in  $i$ .

In the process of the beam transformation to the equilibrium state in the distribution of the current density, additional maxima appear, as

seen in Fig. 4. Unfortunately, the Soviet researchers were not able to investigate the structure of the  $j(\rho)$  maxima near zero, because of the limited number of current cylinders they used in the calculation. However, it is clear the  $j(\rho) \rightarrow \infty$  with  $\rho \rightarrow 0$ . The comparison of the calculated distribution of  $j(\rho)$  and the dependence obtained from the numerical calculations are presented in Fig. 5 [3].

The length of beam relaxation depends to a great extent upon the nature of the initial beam density distribution. Its value is smaller with an inhomogeneous initial distribution and is maximum for an initially homogeneous beam. In the latter case, however, at the start of the coordinates all the electrons have the same betatron oscillation frequency  $\omega_\beta$ , but after passing the point of focus the beam does not remain homogeneous, which leads to the dependence of  $\omega_\beta$  upon the

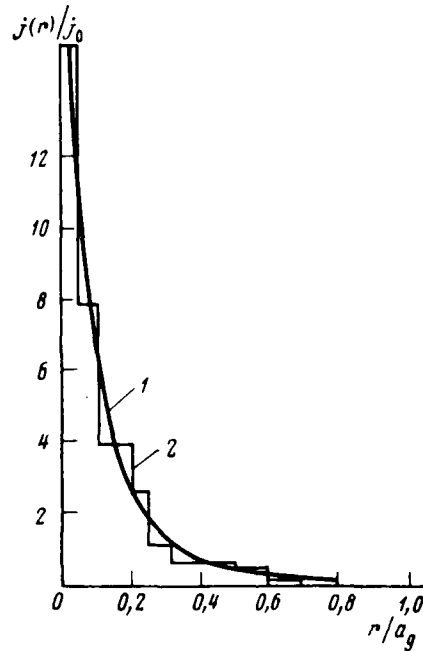


Fig. 5—Comparison of the  $j(\rho)$  distribution normalized to the initial current density  $j_0 = I_b / \pi a_g^2$  with the initial characteristic radius  $a_g$  (curve 1) to the dependence obtained by the numerical calculations (curve 2) [3]

beam radius. For example, with an envelope structure as given in Ref. 7, the beam, after traversing 4 to 5 focusing lengths, begins to spread. However, the researchers have observed a strongly accentuated tendency to the smoothing of the radial density distribution, which shows a gradual striving of the beam to reach the equilibrium state. With an increase in  $i$ , the relaxation length was observed to decrease (as can be seen in Fig. 3).

The beam parameters at the output of an accelerator must be matched to the equilibrium values in effective beam radius as well as in electron distribution in both velocities and coordinates. These conditions, however, are hard to achieve completely. The example as shown above in Ref. 3 does, however, show the possibility of the beam relaxation obtaining an equilibrium state even in the case of incomplete matching of the beam parameters. The results apply to a cold electron beam, but they can also be easily generalized for the case where the electron temperature  $T$  is considerably lower than the equilibrium Bennett temperature  $T \ll T_B = 0.5 \gamma_0 \beta_0^2 c^2 \text{ mi}$ . As mentioned by researchers in Ref. 3, the problem of a collisionless relaxation of a "hot" beam with  $T \lesssim T_B$  has to be considered separately.

Additional work in 1981 was carried out at VEI [8] on the compression of a space-charge-neutralized REB by an external solenoidal magnetic field, taking into account the beam's own magnetic field. For the case of intense REB, it was demonstrated that magnetic field compression has a weak effect upon the beam and can be used only in the case of a beam whose radius at the output of the accelerator is equal to the radius of the beam at the output of the solenoid.

### VEI Experimental Research

Researchers at the VEI Institute performed experiments in 1981 [9] and 1983 [10] on REB transport in low-pressure background gas. These experiments were performed using the 1975 apparatus of Khodatyayev as described in Ref 11. These studies concentrated on the transient processes leading to the formation of a quasi-equilibrium structure of the electron beam in a propagation path free from external magnetic or electromagnetic fields. Measurements were made on the beam-formation time for the quasi-equilibrium state [11], the velocity of the wave front propagation [9], and the beam energy spectra [12]. The most recent study from this research team [10] examined the physical processes that determine the formation of the quasi-equilibrium structure of the neutralized electron beam for long-distance propagation.

The experiments were carried out using a 300 keV injector with a beam current of 100 A, 100  $\mu$ s pulse length, and a beam diameter of 5 cm. The beam drift tube was 10 m in length and 50 cm in diameter, with a magnetic field shield and beam diagnostics that allowed measurement of beam propagation, the distribution of the current density, the radial and longitudinal energy spectra, beam position, and an optically visual beam cross-section. The distribution of the beam current density at distances greater than 50 cm were measured with a graphite collector composed of plates 2 cm wide [11].

The average beam structure as a function of propagation length is shown in Fig. 6 [10] for observation times greater than the transition time to obtain the quasi-equilibrium state of the beam.

A typical oscilloscope trace of the beam collector currents is shown in Fig. 7 at a background pressure of  $5 \times 10^{-5}$  Torr, 300 keV, 70 A, at a distance of  $L = 250$  cm. Curve (1) represents the beam current collected at the center of the beam, while curve (2) represents the beam current collected 4 cm from the beam center. The corresponding increases and decreases of the beam currents in curves (1) and (2) at the beginning of the pulse characterize the process of establishing the quasi-stationary state of the beam.

The size of the beam at the injector anode was determined by the imprint on the anode screen. The beam shapes at the point of focus were determined by using a slit collector with slits 0.2 cm wide. Beyond the point of focus, the beam was found to slowly expand, which is also seen by the slow decrease in the profile of beam amplitude. The average beam profile agrees with that of Bennett distribution, as shown in the insert of Fig. 6, where the calculated Bennett profile is shown by the solid line and the experimental data (the crosses) were obtained by using the collector at  $L = 350$  cm [10].

The transverse beam temperature was measured using collimated luminous targets, as used in Ref. 11 for analyzing the beam structure. At distances close to the focus point ( $L \approx 50$  to 70 cm), the transverse temperature was found to be about 0.5 keV, and at  $L = 350$  cm it was about 2.0 keV. The beam diameter in the vicinity of focus was less than 0.4 cm. At long distances, however, there was no sign of any periodic structures correlating to betatron lengths caused by the beam's own magnetic field.

The reason for such high transverse temperatures was explained to be the existence of collective processes during the interaction of the beam with the background plasma. These processes lead to the formation of waves having low-frequency beam current density oscillations, whose character can be seen by the current scans on the central and outer collectors, as shown in Fig. 7. The average oscillation frequency

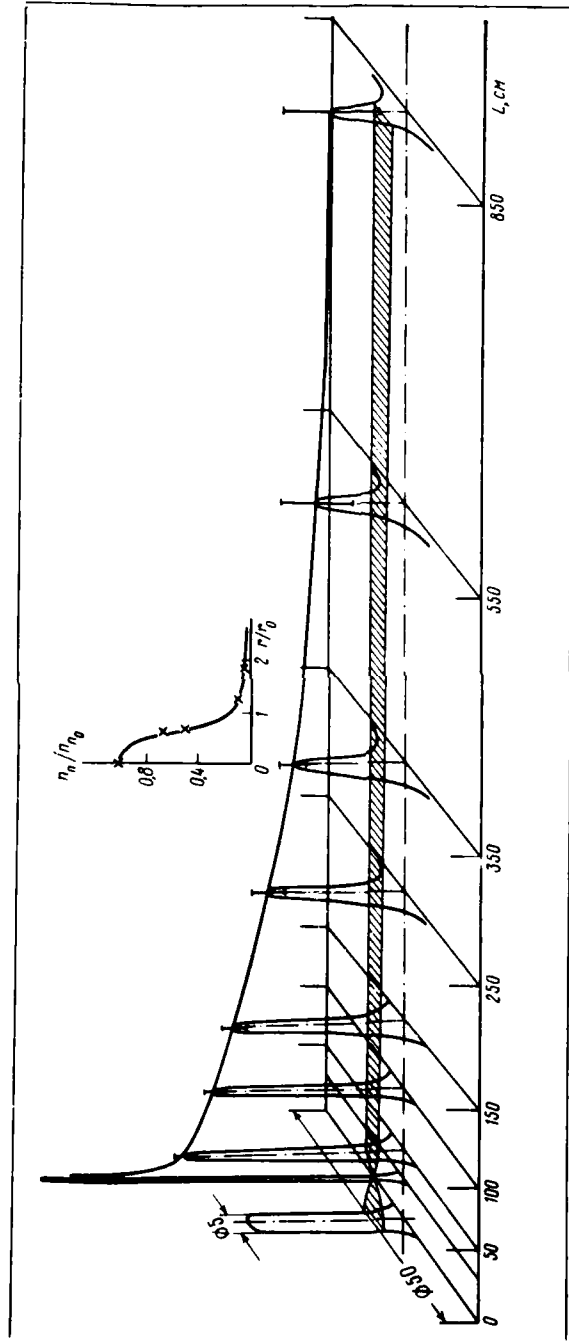


Fig. 6—Average beam structure as a function of propagation length [10]

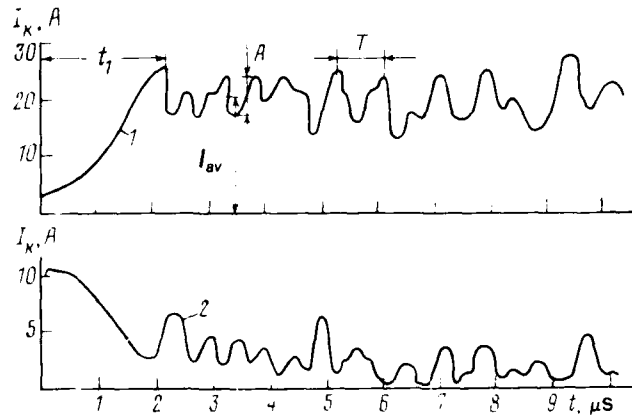


Fig. 7—Oscilloscope trace of the beam current on the (1) central and (2) outer collector plates [10]

has been observed to increase with increasing background pressure and beam current, as illustrated in Fig. 8 [10].

Figure 9 shows the increase of the relative oscillation amplitude as a function of length along the beam for several pressures. Here  $I_{av}$  represents the average oscillation current as shown in Fig. 7.

This dependence corresponds to the oscillations along the beam axis which appear in the vicinity of the electron beam focus. At a distance

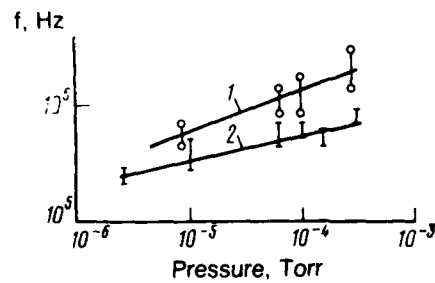


Fig. 8—Dependence of the average oscillation frequency as a function of pressure for different beam currents [10]: curve (1),  $I_b = 50$  to  $70$  A; curve (2),  $I_b = 30$  to  $50$  A



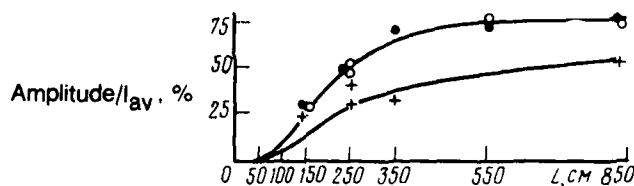


Fig. 9—Relative oscillation amplitude as a function of length along the beam for several different pressures [10];

- :  $p = 10^{-4}$  Torr
- :  $p = 5 \times 10^{-5}$  Torr
- +:  $p = 10^{-5}$  Torr

of  $L = 350$  cm, a saturation of the oscillation amplitude was seen, due to the beam diameter reaching the diameter of the drift tube, thus leading to beam loss to the tube walls.

As observed in Fig. 7, the low-frequency oscillations appear after a certain time  $t_1$ , which has been seen to decrease with an increase in pressure and propagation length. This phenomenon is illustrated in Fig. 10 by the plot of  $1/t_1$  as a function of beam length for several pressures.

At a beam current value of 70 A, the depth of the ambipolar potential well was determined to be about 40 V, as shown in Ref. 11. For this case the plasma density was estimated to be about  $2 \times 10^9 \text{ cm}^{-3}$  for  $p = 5 \times 10^{-5}$  Torr and  $I_b = 70$  A,  $n_0 \sim 2 \times 10^{12} \text{ cm}^{-3}$ . The excitation frequency, corresponding to the maximum values, was found to be 0.1 to 0.5 times the ion plasma frequency with a change in pressure from  $10^{-5}$  to  $10^{-4}$  Torr, which agrees well with the experimental observations as shown in Fig. 8. It was proposed by the VEI researchers that the observed oscillations of the beam current density are caused by the transverse movement of the background gas ions leading to the increase of the transverse beam temperature and, thus, to the increase in beam size. The oscillations appeared only after the formation of the first focus in the beam. This same conclusion was arrived at in 1974 by researchers from IFAN, where the nature of these beam oscillations has also been experimentally investigated [13]. (See the end of Sec. II for more details on this research.)

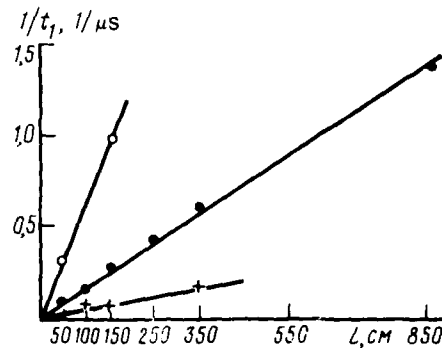


Fig. 10—Dependence of the inverse of the formation time ( $t_f$ ) of oscillations as a function beam propagation length for different pressures [10];

○:  $p = 10^{-4}$  Torr

●:  $p = 5 \times 10^{-5}$  Torr

+:  $p = 10^{-5}$  Torr

It can be observed in Fig. 9 that the low-frequency oscillation amplitudes begin to increase at a certain beam propagation length  $L_c$ . It is in proximity of this length  $L_c$  that it is the easiest to create the conditions to excite waves in the plasma that can effectively interact with the electrons of the beam [10].

It was recently concluded in Ref. 10 that it is quite hard to effectively transport a neutralized, self-focused electron beam over large distances through field free space, mostly because of the spatial increase of the transverse beam energy. In this case the mechanism involved in spreading the beam was identified with scattering, where the role of the scattering centers is assumed not by the particles, but by the field of the transverse oscillating ions whose amplitude, due to the resonance interaction mechanism, increases in the direction of beam propagation. The rate of amplitude increase is determined by the plasma concentration produced by the electron beam. Because of this fact, the VEI researchers state that if one cannot regulate the plasma density one cannot exclude the beam spreading during beam transport [10].

The characteristic electron beam propagation velocities were measured in 1978 in Ref. 9 using a 300 keV, 100 A beam through background air pressures of  $10^{-3}$  to  $10^{-6}$  Torr. The experiments were

carried out using the old apparatus of 1975, as described in Ref. 11. The initial electron beam diameter was 5 cm, while the diameter and length of the drift tube were 50 cm and 10 meters, respectively. The velocity and length of the REB compensating front have been measured and theoretical expressions have been determined. The velocities of the beam along the surface of the drift tube were measured using probes located in the tube walls. The velocities of the compressed beam were determined by a graphite collector located at different distances from the point of injection, using the moment of coincidence of the full injector beam current and the collector currents. The beam profile at different moments in time was determined by using a sectionalized graphite collector placed at different distances along the axis. The beam cross-section intensity was monitored by looking at the intensity of the glow caused by the beam interacting with the background gas at a specific point. The beam glow was measured using a photo multiplier which was shielded against X rays.

Typical oscillogram scans used in the measurements are shown in Fig. 11 [9]. Figure 11a shows the change of the injector accelerator voltage, Fig. 11b the change in the total current of the injector, Fig. 11c a series of oscilloscope traces of the current on the collector located 5 m from the point of injection at various background gas pressures, and Figs. 11d and 11e the current picked up on the ring probes located at 1.5 cm and 5.5 cm, respectively, at a drift tube pressure of  $3.4 \times 10^{-5}$  Torr.

The results of the measurements on the propagation velocity of the REB front in a drift tube at various pressures is summarized in Fig. 12 [9]. The crosses (+) represent the measurements made at the point of electron beam contact with the inner wall of the drift tube. The velocities were measured at maximum collector-beam current and are shown in Fig. 12 for  $P = 10^{-4}$  Torr measured at 0.5 to 8.5 cm (•) and at  $P = 5 \times 10^{-5}$  Torr measured from 0.5 to 3.5 cm (○). Both sets of data show no dependence of velocity upon length along the beam tube. Measurements made with the photomultiplier are shown by ø.

Calculations were also carried out in Ref. 9 in order to obtain a qualitative estimate on the beam propagation process by considering the movement of the compensation front of an axially symmetric beam through the drift tube containing air or gas. The velocity of the compensation front, the characteristic length of the front, and the electron and ion distribution connected with the movement of the front have all been determined.

The calculated values of the compensation front velocity, as computed in Ref. 9, are represented in Fig. 12 by a solid line. Earlier calculations made by researchers from FIAN [14] for the same

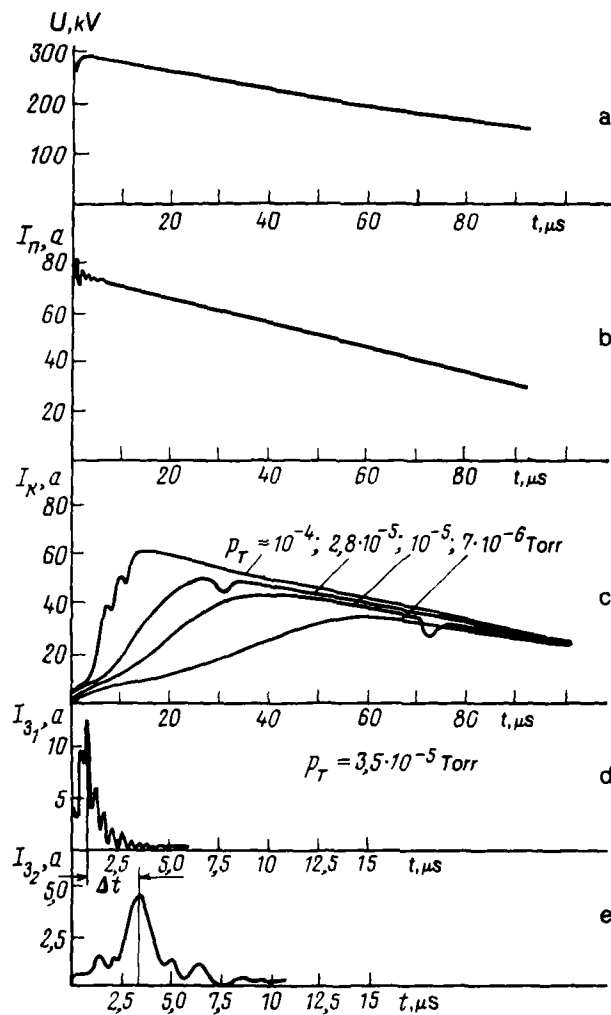


Fig. 11—Oscillograms showing the REB propagation through background gas [9]

- a — injector voltage
- b — injector current
- c — collector current for various pressures in the drift tube
- d and e — current pick-ups on different drift tube wall probes

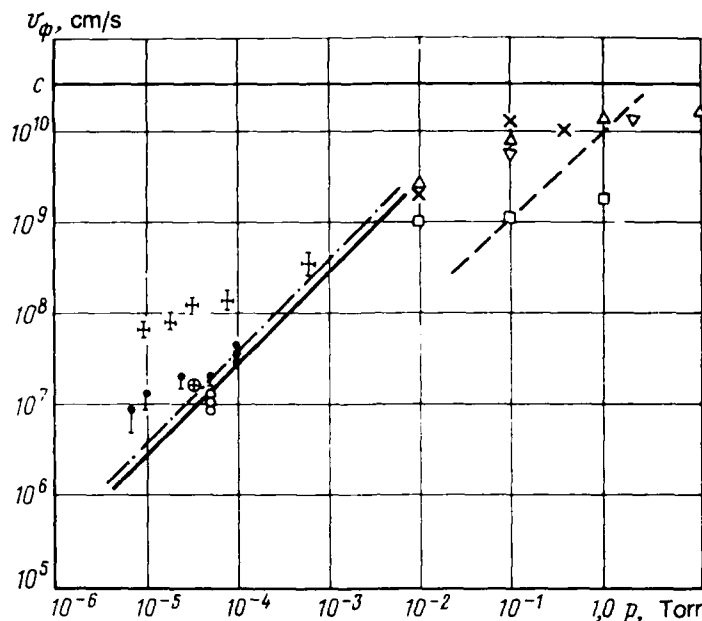


Fig. 12—Velocities of the electron beam propagation as a function of background gas pressure [9]

experimental conditions of Ref. 9 are represented in the figure by the "dash-dot" line, showing good agreement even though two different physical models were used for the calculations. One can also note the good agreement between the calculations and the measurements of the compensation front velocity at  $P = 10^{-4}$  Torr. At the lower pressures, the discrepancy between experiment and calculations becomes larger, probably due to the Soviet researchers' assumed stance of neglecting, in the theoretical model, the effect of the beam front on the ions and their movement. This effect, apparently, is more discernible in the lower pressure range.

The VEI researchers have also included in Fig. 12 experimental data points obtained by other researchers in the pressure range of  $10^{-2}$  to 10 Torr. The work done in 1974 by researchers from the Kharkov Physics-Technical Institute (KhPTI) is shown by ( $\Delta$ ) for a 1 MeV, 40 kA beam in  $N_2$  [15]. The other experimental data were obtained by Western researchers: ( $\times$ ) - 0.4 MeV, 33 kA beam through  $CH_4$  [16], ( $\square$ ) - 0.5 MeV, 40 kA beam through air [17], and ( $\nabla$ ) - 0.4 MeV, 50

kA beam through air [18]. The experimental data, in these pressure ranges, were calculated for the case of ( $\Delta$ ) [15] by researchers from FIAN [14]; they are represented in Fig. 12 by the dashed line.

In 1983 an independent group of VEI researchers under the leadership of M. A. Zavyalov, which specializes in the development of electron guns and electron optics equipment [19, 20] investigated electron beam transport in low-pressure gas with conditions approximating the normal operation of electron guns and injection systems [21]. These experiments looked at the plasma that is created by the electron beam, and the critical values of beam currents and background gas at which point instabilities are initiated. Limits were set on the beam developing the two-stream instability. These investigations, however, were carried out at low beam energies (5 to 30 keV) and low beam currents (0.1 to 3 A), and therefore will not be covered in detail in this report. The interest still lies in the low-pressure range ( $10^{-5}$  to  $5 \times 10^{-3}$ ) Torr and the development of the two-stream beam instability. However, as the electron beam energy is increased, the onset of this instability is pushed into the higher pressure range, which is outside the scope of this report.

### IYaF-TPI EXPERIMENTS

In 1978, IYaF-TPI researchers [22] conducted experiments on the transport of microsecond-pulse electron beams through low-pressure gas ( $P \sim 10^{-4}$  Torr) in the gas-focusing regime. Here the coulomb repulsion was overcome by the forces due to the beam's own magnetic field in the presence of space-charge neutralization of the beam by the background ions. It was demonstrated that, at a pressure of  $\sim 10^{-4}$  Torr, the time necessary for the accumulation of a necessary amount of ions is relatively large (about 1.5  $\mu$ s) [22]. In order to decrease this time it was necessary to speed up the ion accumulation process, which could be accomplished in the following two ways: (1) by increasing the pressure  $P$  in the beam transport channel (within reasonable limits), or (2) by covering the channel walls with an insulator layer. Experiments investigating the transport of electron beams at relatively low pressures have been made in Refs. 22 and 23 for microsecond pulse lengths and in Ref. 24 for nanosecond pulse lengths.

The experimental apparatus is shown in Fig. 13 [22] utilizing the Tonus-2M electron accelerator with a coaxial diode self-insulating type of electron gun. The beam drift tube as well as the electron gun were maintained at a pressure range of  $10^{-4}$  to  $10^{-3}$  Torr. The electron gun demonstrated the most stable operation in this pressure range for microsecond pulse-length range.

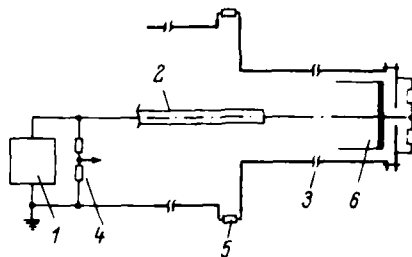


Fig. 13—Electron beam transport experimental apparatus [22]

- 1 — high voltage pulsed generator
- 2 — cathode
- 3 — anode (drift tube)
- 4 — acceleration voltage metering
- 5 — total current shunt
- 6 — faraday cup

The beam transport at the  $10^{-4}$  to  $10^{-3}$  Torr range was experimentally investigated up to a distance of 83 cm in Ref. 23 at an energy of 200 to 250 keV, with beam currents up to 10 kA and pulse lengths of 1.5 to 2  $\mu$ s. The delay time ( $t_d$ ) of the beam pulse as a function of background pressure was investigated and is shown in Fig. 14 [23]. With an increase of pressure from  $8 \times 10^{-4}$  to  $2.8 \times 10^{-3}$  Torr, the delay time  $t_d$  decreased from 1.2 to 0.2  $\mu$ s (a factor of 6). At lower pressures this  $t_d$  decrease is not seen and changes only slightly with an increase in pressure from  $2 \times 10^{-4}$  to  $8 \times 10^{-4}$  Torr.

This can be explained by the effect of gas ionization by the background gas ions. IYaF explains this phenomenon by the fact that, when the REB is injected into the low-pressure gas, a potential well for the ions is formed. The ions, oscillating in this well, provide an additional ionization of the background gas. At higher pressures this process of REB collisional ionization increases but, at the same time, the potential well depth decreases, providing lower ion energy and lower ion effect upon gas ionization. Thus, at the lower pressures when both factors are in effect, the  $t_d$  curve demonstrates a saturation (a plateau) and as one increases the pressure, where the effect of the ions upon the gas ionization decreases, the dependence of  $t_d$  as a function of pressure exhibits an inverse proportional relationship, as shown in Fig. 14 [23].

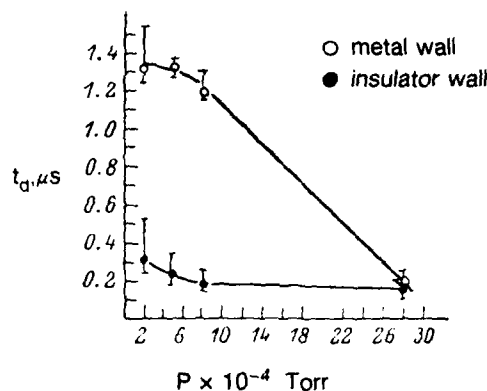


Fig. 14—Beam current delay time measured at the faraday cup ( $L = 32$  cm) as a function of background pressure [23]

When an insulated wall channel is substituted for the metal wall, a substantial decrease in  $t_d$  is seen for electron beam transport, even at pressures of  $2 \times 10^{-4}$  Torr. Any further increase in pressure has almost no effect upon  $t_d$ , as shown in Fig. 14. IYaF researchers have determined that a different means of forming ions is present when transporting an electron beam through an insulated wall channel. An ion cloud is formed due to the ionization of the absorbed gas in the insulator and due to the ion emission from the plasma formed by the bombardment of the channel wall by the electron beam. The decrease in  $t_d$  due to the presence of insulator walls is achieved by the acceleration of the ion formation process, speeded up by the additional neutralization effect of the ions that are freed from the insulator. As seen in Fig. 14, at a pressure of  $3 \times 10^{-3}$  Torr the presence or absence of the insulated channel has almost no effect upon the value of  $t_d$ , which means that the beam achieves full charge neutralization at this pressure.

The effectiveness of the beam transport in a channel is demonstrated by plotting the ratio of the beam current  $I_b$  to the total diode current  $I_D$  as a function of background pressure, as shown in Fig. 15 [23].

The data demonstrate an increased beam transport effectiveness by the introduction of the insulated wall channel. At low pressures of  $2$  to  $8 \times 10^{-4}$  Torr, the presence of the insulated channel increases the  $I_b/I_D$  ratio by a factor of 1.7 due to the increased ionization. At an



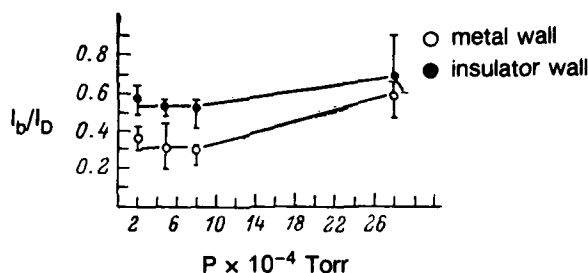


Fig. 15— $I_b/I_D$  ratio as a function of background pressure  
( $L = 32$  cm) [23]

increased pressure of  $3 \times 10^{-3}$  Torr, the ratio increases from 0.6 to 0.7, but at this pressure the presence or absence of the insulated channel no longer has much effect.

However, when the beam transport was investigated as a function of beam transport distance, by observing the beam at distances of 32 cm and 83 cm from the diode, strong defocusing of the beam was observed at the longer distance (at a pressure of  $3 \times 10^{-4}$  Torr). The introduction of the insulated channel and an increase in pressure, however, resulted in a marked improvement of the focusing of the beam and a decrease in the time delay of the beam to reach its target.

It was well demonstrated back in 1972 that intense REB can be well focused and transported through neutral gas at pressures from  $10^{-1}$  to  $10^{-2}$  Torr [25]. At these pressures the space-charge neutralization is accomplished by the ionization of the background gas by the beam itself.

Earlier work at IYaf-TPI on the REB transport through gases at low pressures was published in 1975 [24]. The experiments were carried out in quartz tubes 8 to 9 cm in diameter and 100 cm long using 1.5 MeV, 30 kA, 50 ns electron beams. In these experiments it was determined that the transport of an intense REB through ionized low pressure gas had a sharp dependence upon pressure without any external magnetic fields. This dependence can be seen from the experimental data of  $I_b$  output as a function of gas density, as shown in Fig. 16 [24].

It can be seen in Fig. 16 that at the point of insufficient space-charge neutralization (represented by the left-hand side of the curves),

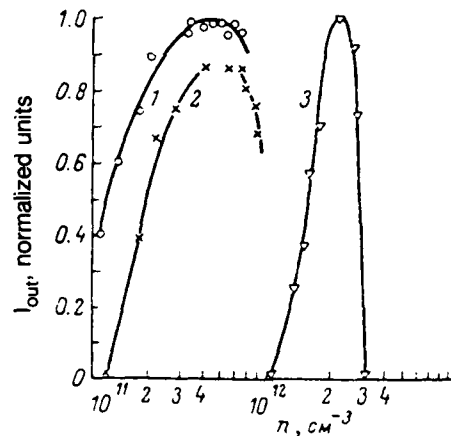


Fig. 16—Dependence of beam current (at the output of the drift tube) as a function of plasma density [24]

○:  $n_e = 6.6 \times 10^{10} \text{ cm}^{-3}$ , 0.4 MeV, 5 kA, 30 ns

$d = 9 \text{ cm}$ ,  $B_0 = 80 \text{ Oe}$

×:  $n_e = 6.6 \times 10^{10} \text{ cm}^{-3}$ , 0.4 MeV, 5 kA, 30 ns

$d = 9 \text{ cm}$ ,  $B_0 = 125 \text{ Oe}$

▽:  $n_e = 2.3 \times 10^{11} \text{ cm}^{-3}$ , 1.5 MeV, 30 kA, 50 ns

$d = 8 \text{ cm}$ ,  $B_0 = 95 \text{ Oe}$

the beam showed poor transport capability. At the optimum transport pressure, a strong self-focusing of the beam was observed at the input and output of the drift tube [24]. At higher pressures (as shown by the right-hand side of the curves in Fig. 16), the transport efficiency decreased and the beam diameter was seen to increase at the output of the beam tube.

When an external magnetic field was imposed upon the beam, the transport efficiency decreased. The Soviet researchers explained this phenomenon by the fact that, as the plasma density radial distribution increases in non-uniformity, the space-charge neutralization at the beam periphery becomes insufficient.

The researchers have shown that REB transport through preionized low-pressure gas can be achieved with careful choice of background pressures.

## LGU IONOSPHERIC MODELS

Leningrad State University (LGU) focused its research on the IREB transport specifically at high altitudes above the earth [26, 27]. The analysis involved the parameters of a nondivergent equilibrium IREB, beam stabilization by polarized ionospheric plasma, and the effect of electron concentration, at various altitudes for day and night temperatures, as well as the effect of the earth's magnetic field. It was demonstrated that in the area of maximum electron concentration in the ionosphere, IREBs can be propagated with currents greater than 1 MA. The analysis of beam self-focusing due to compression of background plasma ions by the beam electric field showed that the resulting increase in current density is limited by hose instability in the beam [27].

Since the daytime electron concentration at a given height varies considerably, the current density of the equilibrium beam must also vary. In addition, electron concentration may drop substantially during the night to a point where the earth's magnetic field will play an equally important part in stabilizing the beam.

The authors considered a cylindrical monoenergetic IREB injected into a rarefied plasma parallel to the earth's magnetic field during time  $\tau$ , with an electron plasma density  $N$  much less than the electron beam density  $n_b$  ( $n_b \gg N$ ). The passage of the beam causes a high polarization of atmospheric plasma because the beam electric field removes plasma electrons from the beam path. The plasma electrons are removed either by the electric field in front of the beam or by the internal electric field of the beam front. The analysis reported in Ref. 27, involving highly localized flows, found only the latter case to be true, when the beam pulse length  $\tau$  is considerably longer than the characteristic time  $\tau_e$  for the repulsion of the electrons.

The same analysis also showed that as the plasma electron is displaced from the beam axis to its boundary, it is accelerated to  $E = 30 I$  eV, where  $I$  is the total beam current in amperes. From this expression it can be seen that, for a beam current of 100 kA, plasma electrons would be accelerated inside the beam to energies of several MeV.

In a system where  $\tau \gg \tau_e$ , the electric field of the leading front of the beam forces out plasma electrons from the beam path, and the space charge of the main body of the beam is partially neutralized by the positive charge of the plasma ion component. If, however, the beam pulse length is  $\tau \ll \tau_i$ , where  $\tau_i$  represents the characteristic time required to compress the plasma ions, during the beam propagation process the plasma ions remain unmoved and one can use a partially compensated beam model with stationary background ions [28].

When the beam pulse is  $\tau \geq \tau_i$ , the background ions become trapped in the potential well of the beam, increasing the neutralization of the beam's space charge and the lateral limitation of the beam.

LGU analyzed the specific case of an IREB emerging from the injector and propagating through high-atmosphere plasma without much beam spreading. It was assumed for this case that  $\tau_e \ll \tau \ll \tau_i$ .

Data on electron concentration in the upper atmosphere were taken from the Canadian Alouette satellite measurements [29]. These data are presented in Table 1 for maximum electron concentration  $N_{\max}$  during the day, and minimum electron concentration  $N_{\min}$  at night, for altitudes from 300 to 1030 km.

LGU showed that the maximum current density for an equilibrium beam at a certain altitude was dependent only upon the local maximum value of electron concentration. This beam current density was expressed by:

$$j \approx 5.3 \times 10^{-9} \beta (1 + 2E_b)^2 N \text{ A/cm}^2$$

Here,  $E_b$  is the kinetic energy of beam electrons (in MeV),  $N$  is the electron concentration in plasma,  $\beta = v/c$ , and the beam injection time is

$$\tau \gg \tau_e^{\text{eq}} \approx 4.4 \times 10^{-5} \beta^{-1} (1 + 2E_b)^{-1} N^{1/2} [\text{c}]$$

The current density of an equilibrium beam was expressed, taking into account the geomagnetic field, as follows [27]:

Table 1

ELECTRON CONCENTRATION IN  
THE UPPER ATMOSPHERE

Altitude (km)	$N_{\max}$ , $\text{cm}^{-3}$	$N_{\min}$ , $\text{cm}^{-3}$
300	$3 \cdot 10^5$	$3 \cdot 10^4$
400	$10^5$	$2 \cdot 10^4$
500	$7 \cdot 10^4$	$10^4$
600	$5 \cdot 10^4$	$6 \cdot 10^3$
700	$3 \cdot 10^4$	$4 \cdot 10^3$
800	$2 \cdot 10^4$	$3 \cdot 10^3$
900	$2 \cdot 10^4$	$2 \cdot 10^3$
1030	$10^4$	$8 \cdot 10^2$

SOURCES: Ref. 27, 29.

$$j^{eq} \approx 4.5 \times 10^{-5} \beta (1 + 2 E_b) H^2 + 5.5 \times 10^{-9} \beta (1 + 2 E_b)^2 N$$

Here,  $j^{eq}$  is the equilibrium beam current density in A/cm<sup>2</sup>, and H is the geomagnetic field in oersteds. (The superscript eq specifies an equilibrium beam.)

The value of electron concentration at an altitude of 200 to 400 km during maximum sun activity reaches  $3 \times 10^6$  cm<sup>-3</sup>. Parameters of an equilibrium IREB calculated for  $N = 3 \times 10^6$  cm<sup>-3</sup> are shown in Table 2. Here, values are shown for beam energy,  $E_b$ , beam current density,  $j^{eq}$ , time required to form space-charge neutralization,  $\tau_e^{eq}$ , power density of the equilibrium beam,  $P^{eq}$ , total beam current,  $I_b$  for beam radii of 10 and 100 cm, and the time required to compress the ion plasma core,  $\tau_i^{eq}$ .

As can be seen in Table 2, high values of IREB currents can be transported through the ionosphere in the area of maximum electron concentration. The current in an equilibrium beam having a radius of 1 meter can be higher than 10<sup>6</sup>A for an electron energy higher than 22 MeV. The attainable power densities can be higher than 1 GW/cm<sup>2</sup> for electron energies higher than 25 MeV [26].

LGU has also found that various beam instabilities can arise during self-focusing of the equilibrium IREB. If the formation time of the instability with a certain wavelength becomes less than the self-focusing time, then beam focusing terminates, producing the given instability. The Budker instability [30, 31] has been considered in Ref. 27, analyzing instability in the entire space-charge neutralized beam, including the flow of positive ions and the restraining electro-static

Table 2  
PARAMETERS OF AN EQUILIBRIUM IREB FOR PLASMA  
ELECTRON CONCENTRATION  $N = 3 \times 10^6$  cm<sup>-3</sup>

$E_b$ , MeV	$j^{eq}$ , A/cm <sup>2</sup>	$\tau_e^{eq}$ , ns	$P^{eq}$ , MW/cm <sup>2</sup>	$I_b$ , kA (R = 10 cm)	$I_b$ , kA (R = 100 cm)	$\tau_i^{eq}$ , ns
1	0.13	9.1	0.13	0.014	4.1	1000
5	1.9	2.3	95	0.59	59	260
10	7	1.2	70	2.2	220	140
20	27	0.62	540	8.5	850	70
30	59	0.42	1800	18.5	1850	47
40	100	0.31	4200	33	3300	36
50	160	0.25	8100	51	5100	28

SOURCES: Refs. 26, 27

forces. LGU found that the long-wavelength instabilities, with  $\lambda \sim L$  (where  $L$  is the length of the beam), are the first to arise.

According to LGU, a high current of  $10^6$  A with a 1 meter radius is not readily obtained in practice. It is easier to consider a nonequilibrium beam that expands to a maximum radius  $r_{\max} \sim 1$  m. In one case, LGU researchers showed that the nonequilibrium beam current amounts to 19.5% of the total equilibrium beam current. Thus the current of nonequilibrium beams is still large enough, reaching  $10^6$  A at 50 MeV [27].

LGU has also calculated the limit of beam propagation distance. The analysis assumed an IREB in the plane of geomagnetic equator ( $\psi = 0^\circ$ ) at an altitude of 300 km, beam energy of 2 MeV, beam radius about 1 meter, with the beam injected along pitch angles of  $\alpha = 45^\circ$  and  $\alpha = 0^\circ$  (along the earth's magnetic field). For both pitch angles, the maximum distance of propagation ( $L$ ) was less than 4.3 km.

In a second case, a geomagnetic latitude of  $\psi = 60^\circ$  was assumed, with all the other parameters remaining the same. With lateral injection,  $L$  was less than 11 km for  $\alpha = 0^\circ$ , and less than 1.5 km for  $\alpha = 45^\circ$  [27].

Besides the theoretical work on IREB propagation at high altitudes, the LGU research group was involved in theoretical analysis of beam injection into plasma [32], plasma dynamics [33, 34], and satellite dynamics studies [35, 36].

## IFAN LOW CURRENT EXPERIMENTS

A team of researchers at the Physics Institute of Kiev (IFAN) has published a number of experimental papers on electron beam transport through low-pressure gas ( $10^{-5}$  to  $10^{-3}$  Torr). This work, however, was performed using relatively low voltages (up to 20 kV) and currents (in the mA and A range) and therefore is mentioned here only in passing.

This IFAN research included the observation of ion oscillations generated by the passage of an electron beam in free space [13], the formation of quasi-stationary waves excited by electron beam pulses in background plasma [37, 38, 39], phase focusing of a density-modulated electron beam [40], self-focusing of a neutralized beam [41, 42, 43], and the combination of electron and positive ion beams [44].

### III. IREB PROPAGATION EXPERIMENTS UTILIZING INSULATED CHANNELS

Research on the use of insulated wall channels for the transport of intense REBs at low pressures has been recently carried out at four different institutes: FIAN, OIYaI, YeGU, and IYaF-TPI. The researchers at FIAN, YeGU, and IYaF-TPI looked at the effect of insulated channels upon the parameters of the beam, and the optimum conditions for beam transport over long distances in the background gas-pressure range of about  $10^{-5}$  Torr. The researchers at OIYaI concentrated only on developing the plasma channel that is formed inside the insulated wall metal pipe, but have not yet published any results on the effect of this channel on the individual beam parameters and the overall transport of the IREB. OIYaI researchers claim the development of an insulated channel with the wall plasma controlled independently from the REB that passes through the channel. The plasma created at the wall of the insulated channels used by FIAN and YeGU researchers is created by the beam that is passed through the center of the channel and is therefore dependent upon the changing characteristics of the electron beam.

The research carried out at IYaF-TPI on the use of insulated channels has been included together with the IREB propagation studies previously described in Sec. II, and therefore will not be repeated here.

#### FIAN RESEARCH

The earliest Soviet research on the IREB transport through insulated channels was done in 1977 at FIAN [45]. The wall plasma was formed by the passage of an 800 keV, 30 kA, 50 ns pulsed electron beam through the center of the insulated channel at a pressure of about  $5 \times 10^{-5}$  Torr. The experimental results of these investigations are shown in Fig. 17 [45].

It is seen from the figure that with the use of a metal channel, the beam is only 35 percent of the injected beam at a distance of 5 cm, and is practically zero at 10 cm. However, with the insertion of the insulated channel, the beam transport is increased dramatically. At the end of the channel, the beam pulse was found to have a shorter pulse front and a shorter pulse length, as demonstrated by curve 4 in Fig. 17. At a distance of 10 cm, the front was observed to be shortened by a

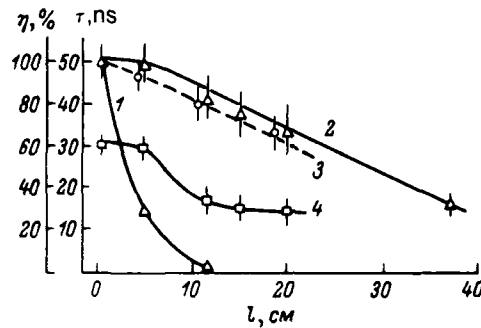


Fig. 17—Beam propagation through the insulated wall channel as a function of channel length [45]

1 —transport efficiency  $\eta = \frac{I_b}{I_{inj}}$  through metal channel

2 —transport efficiency  $\eta = \frac{I_b}{I_{inj}}$  through insulated channel

3 —charge transport efficiency  $\eta_Q = \frac{Q_b}{Q_{inj}}$  through insulated channel

4 —change in pulse length of beam front

factor of two and beyond it remained unchanged. The researchers stated that at longer distances the beam keeps away from the walls and propagates close to the channel axis. With an insulated channel of 3.8 cm inside diameter, the electron beam was about 2.8 cm in diameter.

As stated in Ref. 45, at low pressure of the background gas, the formation of the required number of ions for space-charge neutralization of the beam in the channel is not possible. Therefore, these ions must be extracted by the electric field of the beam from the plasma formed at the insulator wall of the channel. For an injection voltage of 400 kV the time required for protons to travel from the plasma to the beam was calculated to be 2.5 ns, showing that the time for the ions to penetrate the beam is sufficiently short.

An experiment demonstrated that the surface discharge on the insulator wall is the prime mechanism in the plasma formation. The electron beam was able to be propagated even along bent insulated



channels without any beam loss. In these experiments, IREB transport through the insulated channel was made possible by the effect of losing part of the beam electrons to the formation of the wall plasma, creating the condition for the beam transport. The basic beam energy loss was found to take place at the beam front. The shortening of the pulse front can be used for the formation of beams with fast current buildup. The beam focusing mechanism in the case of the insulated channel was found to be analogous to IREB transport through low pressure gas.

The latest experimental and theoretical research at FIAN on IREB transport through insulated channels was made in 1981 [46] with an IREB of 350 to 800 keV energy and beam current up to 100 kA, using the "IMPUL's" accelerator as described in Ref. 47. The experimental apparatus is shown in Fig. 18. Insulated channels used in the tests varied from 5 to 40 cm in length and 2 to 10 cm in inside diameter.

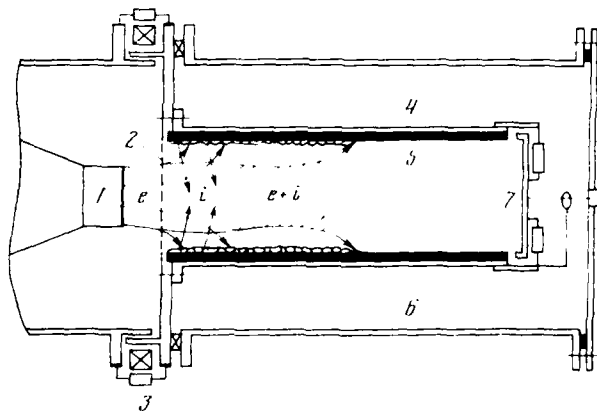


Fig. 18—Schematic of the experimental apparatus [46]

- 1 —cathode
- 2 —anode screen
- 3 —current shunt of Rogowski belt
- 4 —return current conductor
- 5 —insulated channel
- 6 —vacuum chamber
- 7 —faraday cup

Figure 19a shows the effective beam transport efficiency as a function of insulated and metal channel length, for a channel with an inside diameter of 3.4 cm.

As shown in the figure, the effective beam transport efficiency in the insulated channel case is sufficiently high, while in the metal channel the beam is almost completely lost at a distance of 10 cm. The output beam current delay time is dependent upon channel length, as shown in Fig. 19b, and is the same for both insulated and metal channels. It was also determined in these measurements that, inside the insulated channel, an equilibrium beam diameter is reached within a few centimeters; it remains constant along the beam axis and is independent of the diameter of the injected beam (independent of cathode diameter) as demonstrated in Fig. 20 [46]. The equilibrium beam diameter as a function of beam current is shown in Fig. 21. Here the experimental data are compared for the case of an insulated channel with theoretical calculations.

The relationship of the channel diameter to the input beam diameter was shown to have an effect upon the effective beam transport. The effective beam transport efficiency through a 20 cm insulated

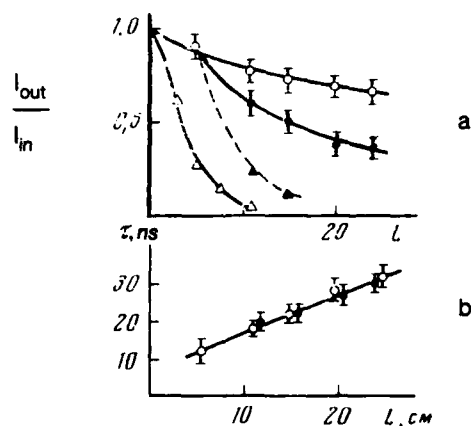


Fig. 19—The effective beam transport efficiency  $I_{out}/I_{in}$  and the output beam current delay ( $\tau$ ) as a function of channel length [46]

- —insulated channel
- —5 cm long insulated channel followed by metal channel
- ▲ —metal channel separated from the insulated insert by a 50 micron titanium foil
- △ —metal channel

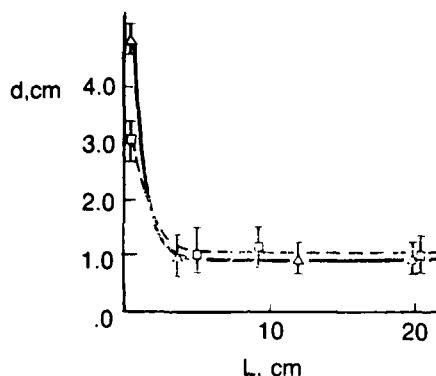


Fig. 20—The IREB equilibrium diameter formation in an insulated channel of length  $L$ . Beam injection voltage 500 kV, beam current 5 kA [46]

Solid line — 4.4 cm diameter cathode  
Dashed line — 2.5 cm diameter cathode

channel is plotted in Fig. 22 for different ratios of the equilibrium beam diameter to the cathode diameter (input beam diameter). A well-defined maximum is seen here for a ratio of close to one of the specific equilibrium beam diameter to input beam diameter.

The beam delay time and effective transport efficiency were found to be independent of the insulator material of the channel walls. The use of insulated channels made from different materials (such as plexiglass, polyethylene, glass, and quartz) produced absolutely no change in operation. The Soviet researchers stated that the lack of any effect is due to the plasma that is formed from the adsorbed layer on the insulator surface. The composition of the plasma, which is primarily determined by vacuum pumping properties, is the same for all of the different channel inserts. Thus, the insulator itself does not participate in the formation of the plasma and acts only as a charged surface support.

In the beam transport through the insulated channel, the leading front of the beam pulse was seen to be lost, as demonstrated in the oscilloscope trace of the beam current pulse at the channel input and output (Fig. 23).

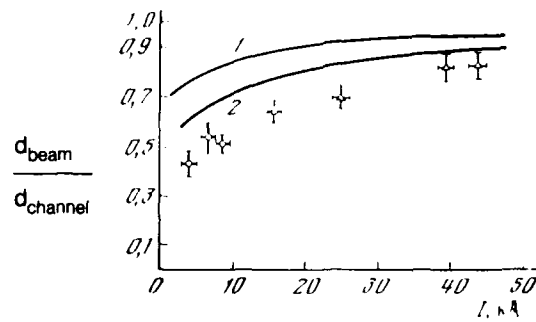


Fig. 21—IREB equilibrium diameter as a function of beam current for beam transport through an insulated channel [46]

—500 keV beam

$\Delta$ —400 keV beam

Theoretical calculations: Curve 1 —  $\gamma = 1.5$

Curve 2 —  $\gamma = 2.0$

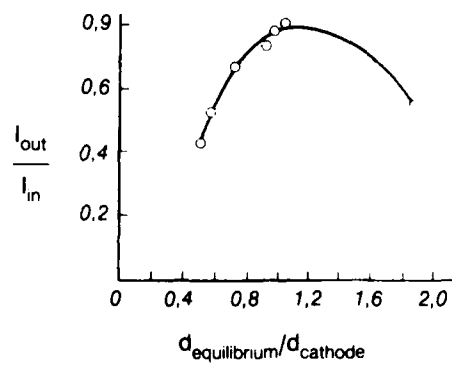


Fig. 22—The effective beam transport efficiency  $I_{\text{out}}/I_{\text{in}}$  through a 20 cm long insulated channel for different ratios of the equilibrium diameter to cathode diameter [46]

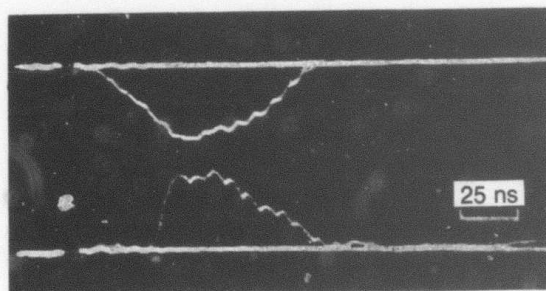


Fig. 23—Beam current pulse injected into the channel (top curve) and at the output of the channel (18 cm long and 3.4 cm in diameter) [46]

The minimal delays at short distances from the anode were about 5 to 10 ns and did not depend upon beam current, energy of the electrons, or the channel diameter. The pulse delay at the exit of the channel was dependent upon the channel length, as previously mentioned and shown in Fig. 19b.

Measurements were also made of the ions flowing in the beam by using a faraday cup at the end of the channel and by deflecting the electron beam with a transverse magnetic field. The energy of the ions was measured by using a time-of-flight spectrometer, with the first spectrometer collector (a steel 70 percent transmission screen) located 75 cm, and a second collector located 100 cm, from the end of the channel. The ion current pulses as measured on the collectors are shown in Fig. 24, showing a spread in the ion velocities or a multicomponent composition of the ion beam. The time delay, which depended upon the diode voltage, agreed well with the time-of-flight of protons having energy equal to that of the electron beam [46].

The FIAN researchers in Ref. 48 found that the protons created in the insulated channel had two different energy ranges. The major group had energy near to or slightly less than that of the electron beam, and a second group had three to five times the energy of the electron beam. Their tests have demonstrated, however, that these protons are accelerated not only within the confines of the insulated channel, but also beyond it.

From the analysis of equilibrium relativistic electron beams, the FIAN researchers claim that beam transport through insulated channels is not limited in beam current. However, in their experiments they have observed that, when using a small enough diameter channel,

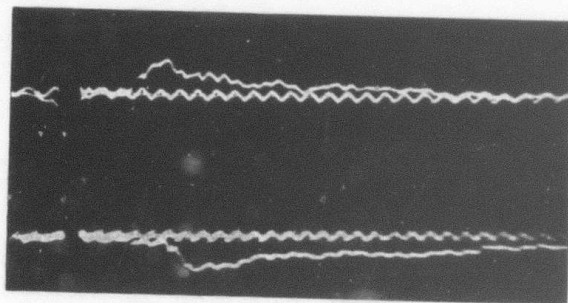


Fig. 24—Ion current pulses on collectors located 75 cm (top) and 100 cm (bottom) after the insulated channel; the calibration frequency used is 100 MHz [46]

the beam filled the channel completely; and upon further reduction of the channel diameter, there was no observed increase in the beam current density. One of the possible limitations of beam focusing in the insulated channel is the limitation of the ion density emitted from the wall plasma. In fact, the REB focusing requires the ion density increase to be inversely proportional to the channel diameter. Thus, a decrease in channel diameter requires a practically unlimited ion emission from the wall plasma. The increase of this emission from the plasma can be accomplished by increasing its density and temperature, which is done by impinging an additional part of the REB into the wall of the insulator channel. In order to verify this postulate, the researchers carried out experiments using a 600 keV, 80 kA, 1.7 cm diameter electron beam, which they injected into a 30° conical insulated channel with an input diameter of 2 cm and an output diameter of 0.6 cm. The beam amplitude at the exit of this channel was only 30 kA, providing an average current density inside the channel of 100 kA/cm<sup>2</sup>. Another channel, using three separate insulated conical sections, with an input diameter of 5.1 cm and an output diameter of 1.7 cm, was used for comparison. Results of this experiment are shown in Fig. 25 [46].

In the larger-diameter case, the transport efficiency is seen to increase dramatically as soon as the plasma due to the electrical discharge at the wall is formed and then to fall off because of the spacing between the three sections of the conical channel. In the smaller-diameter case, the transport efficiency increases gradually because of the increase in beam current introduced into the chamber wall and thus the corresponding increase in temperature and emission from the

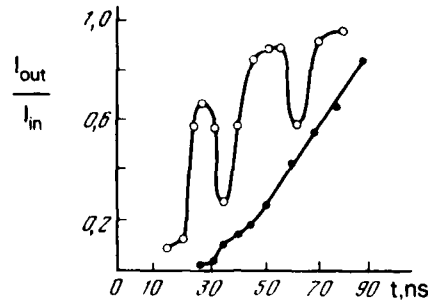


Fig. 25—Effective beam transport efficiency as a function time for a conical insulated channel [46]

- —2.0 cm input diameter, 0.6 cm output diameter
- 5.1 cm input diameter, 1.7 cm output diameter

wall plasma, finally reaching a maximum value at the end of the current pulse. It is thus evident from these measurements that control and optimum production of the ion emission from the plasma is required for optimum neutralization of the REB. The FIAN researchers admit to not fully understanding the mechanism involved in the trapping of the ions by the electron beam and the ion flow in the direction of the beam. They have demonstrated, however, that for efficient beam transport it is necessary to match the channel geometry with the beam at the input to the channel. This means that the diameter of the injected beam must be close to the equilibrium beam diameter. For the case of conical-shaped channels, the angle of the cone of the insulated channel has to correspond to the angle of the injected electron beam.

In 1981, researchers at FIAN also investigated the use of an insulated channel with "needles" mounted into its inner surface in order to facilitate surface breakdown and reduce the asymmetry of surface plasma formation [48]. These needles, fabricated from copper and 2 mm in diameter, were placed at 1 cm intervals in the inner walls of the insulated channel, and were connected to a copper liner on the external surface of the channel and joined to the anode. The beam front velocity in the "needle" channel case showed an increase by a factor of four over the smooth-wall-channel case, reaching  $4 \times 10^9$  cm/s. The beam current transport efficiency, however, was found to be less in the needle channel case, probably because of the absence of a return current inside the plasma. When there is an absence of a return current in the plasma (since in this case the return current flows in the

external copper-liner circuit), there is no additional heating of the plasma and, therefore, the plasma emits fewer ions [48].

In subsequent tests, these researchers also investigated the effect of different distribution of the return current flow through the insulated channel and its effect upon the cross-sectional shape of the REB. The return current was made to flow through two-wire and four-wire conductors near the inside wall of the insulated channel. In the case of the return path for two wires 180° apart, the REB was found to possess a disk-shaped cross-section, demonstrating quadruple focusing. In the case of the evenly spaced, four-wire return path, the REB was found to possess a star-like cross-section, demonstrating octuple focusing.

### YeGU RESEARCH

The research at YeGU was carried out in 1981-1982 using a 400 keV, 20 kA, 30 ns electron beam injected into an insulated wall channel at gas pressures of about  $10^{-5}$  Torr. Measurements were made to determine the effect of the channel length upon the beam dispersion angle at the output of the channel. The dispersion angle was determined by using quartz tubes located at different distances within the channel and by observing the beam images formed on the tubes at various distances along the beam path length. The dispersion was found to vary from 45° at the entrance of the channel to 15° at a distance of 50 cm along the beam length, as shown in Fig. 26 for a channel diameter of 4.2 cm and a beam current of 20 kA at the channel entrance [49, 50].

Another series of measurements made by YeGU researchers was carried out in order to determine the optimum utilization of the insulated channel in the passage of the REBs. Immediately beyond the anode grid, in these experiments, a copper tube was mounted in which insulating channels of various lengths could be inserted. The insulating channel materials used in these experiments were glass, quartz, dacron, polyethylene, and teflon, with channel diameters of 4.2 cm and wall thicknesses of about 1 mm. Sectioned faraday cylinders and phosphorescent detectors were used to determine the beam diameter and beam current density along the axis of the channels as a function of distance from the anode, as well as the distribution of the current density as a function of beam radius at the exit of the channel, as shown in Figs. 27 and 28 [49].

As seen from the figures for a metal channel, the beam reaches a minimum radius showing self-focusing of the beam at a distance of 10 mm from the anode. Beyond this the beam expands; and at a distance



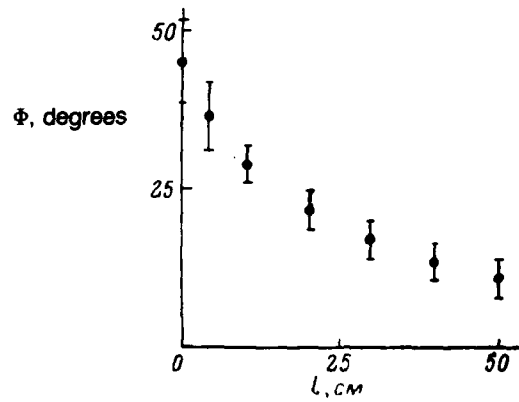


Fig. 26—Dependence of the IREB dispersion angle upon the transport length within an insulated channel of 4.2 cm diameter [49]

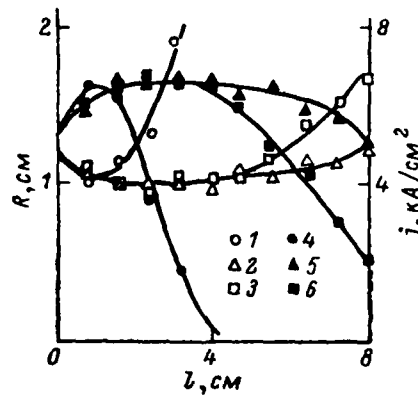


Fig. 27—Dependence of the beam radius (curves 1-3) and beam current density along the beam axis (curves 4-6) as a function of distance along the channel. Copper channel of 80 mm length (1, 4) and insulated channels of 80 mm length (2, 5) and 40 mm length (3, 6) [49]

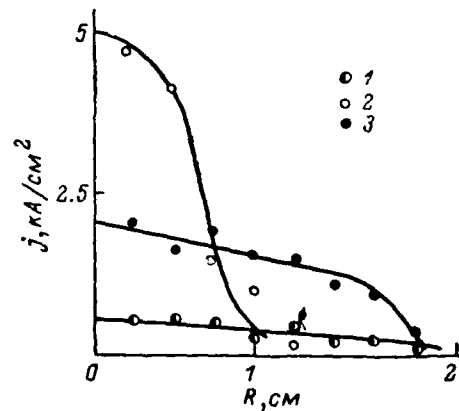


Fig. 28—IREB current density distribution along the beam cross-section at the output of the transport channel [49]

- 1 —copper channel
- 2 —insulated channel,  $L = 80$  mm
- 3 —insulated channel,  $L = 40$  mm

of about 40 mm from the anode, the beam radius becomes equal to the radius of the metal tube and the beam current density on axis drops to  $1 \text{ kA/cm}^2$ . At the channel output the beam is relatively homogeneous, but the total current is only 4 kA.

When the insulated channel is inserted into the metal channel, the beam current density on axis reached about  $5 \text{ kA/cm}^2$  and the total beam current at the exit of the channel reached 18 kA, but the current density distributions along the radius were quite inhomogeneous.

The use of different insulator materials showed no observed effect upon the REB propagation, but showed a marked effect upon the operational lifetime of the insulator channel. The lifetime (in relative units) was determined as follows [49]:

Material	Relative Lifetime
Polyethylene	1
Dacron	3.2
Teflon	9
Glass	15
Quartz-glass	22

The experiments as recently carried out at YeGU [49, 50] have thus demonstrated the ability to improve the beam propagation parameters by using insulated transport channels. By varying the length of the channels, it is possible to control the value of the beam dispersion angle. It was also determined that, by varying the length of the insulated channel inside the conductor channel, it is possible to rearrange the beam current density along the beam radius and obtain a reduced density (up to 2.5 times lower) that can facilitate the condition of material choice between the vacuum diode and drift space.

The most recent experiments on the optimization of IREB transport through insulated channels was made at YeGU in 1983 [51] using the accelerator as described in Ref. 49 with a beam energy of 400 keV, beam current of 20 kA, and pulse length of 30 ns. In these experiments, investigations were made into optimum choices of background gas pressure and type of gas, and details of the construction of the insulated channel. However, transport through the insulated channel was carried out at background air pressures from 0.1 to 50 Torr, which is outside the pressure range considered in this report. These experiments are briefly mentioned here since they are a continuation of the investigations made at the low-pressure range and are of prime interest.

The optimum beam transport was found at a pressure of 2 Torr for an insulated channel 1.2 m long, mounted inside a conducting tube that carried the return current. This optimum beam transport was observed for the condition where the total current had a minimum value (here  $I_T = I_b + I_{P1}$ , where  $I_b$  is the beam current, and  $I_{P1}$  the reverse current of the plasma electrons).

The schematic of the experiment is shown in Fig. 29 [51].

The results of interest for air propagation are depicted in Fig. 30, showing the transport efficiency  $I_{tr}/I_o$  (ratio of beam current transported to the beam current input to the channel) as a function of pressure [51].

As can be seen from Fig. 30, the use of the insulated channel expands the range of optimum air pressure towards the low-pressure end (0.1 Torr and below). From these measurements, the YeGU researchers concluded that optimum beam transport can be achieved with the use of an insulated channel mounted inside a current-carrying metal tube. Surrounding the insulated channel by the metal tube increases the channel's capacitance as well as the density of the plasma formed at the insulator wall, and thus increases the transport efficiency,  $I_{tr}/I_o$ . The researchers mentioned that this same mechanism also helps beam transport at the higher pressures because, owing to the fast dissipation of the reverse current of the plasma electrons ( $I_{P1}$ ), the

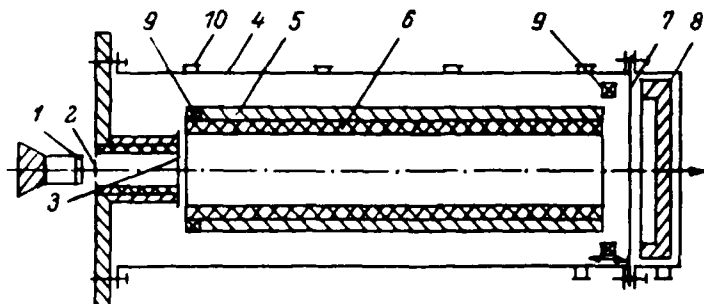


Fig. 29—Schematic of the experimental apparatus [51]

- 1 —cathode (diameter 3.6 cm)
- 2 —anode (screen with 70% transmission)
- 3 —steel foil (20 microns thick)
- 4 —copper tube (1.3 m long, 9 cm diameter)
- 5,6 —insulated channel drift tube components (1.2 m long)
- 7 —metal foil
- 8 —faraday cup
- 9 —Rogowski belts
- 10 —vacuum windows (for spectral plasma observations)

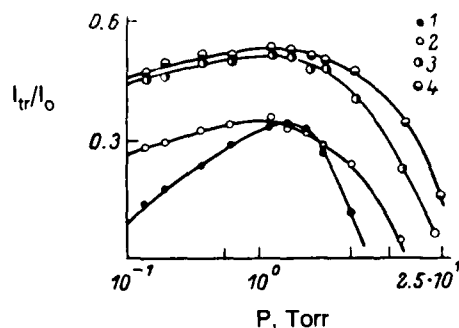


Fig. 30—Dependence of transport efficiency ( $I_{tr}/I_0$ ) upon background air pressure for different transport channels [51]

- 1 —metal channel, 3.6 cm ID
- 2 —insulated channel, 3.6 cm ID
- 3 —insulated channel, 3.6 cm ID inside a return current conducting cylinder
- 4 —insulated channel, 9.0 cm ID inside a return current conducting cylinder

beam current neutralization weakens and the beam expands to the edges of the channel walls, at which point the wall plasma provides additional beam neutralization. In the higher pressure range, at the optimum pressure value of about 2 Torr, the beam was observed to be localized close to the beam axis and the wall plasma had only a weak effect upon the beam transport mechanism.

The YeGU researchers state that the main problem of beam transport at the lower pressure range is the sharp increase in the time required to obtain beam neutralization. For this lower pressure case, they recommend further research on the use of a prepared high-density plasma for the effective neutralization of the electron beam.

Researchers at YeGU also carried out experiments in 1982 on IREB transport through curved insulated channels with 3.3 cm inside diameter and 26 cm long, using a 300 keV, 20 kA, 30 ns electron beam [52]. With a channel beam axis radius of 50 cm, the beam current at the exit of the channel was found to decrease by only 2 percent. With a channel beam axis radius of 25 cm, however, 24 percent of the beam current was lost.

## OIYal RESEARCH

The research represented by OIYal involves the development of a plasma channel set up inside an insulated-wall metal pipe. In 1982 the OIYal researchers demonstrated the formation of a homogeneous plasma along the surface of an insulated cylinder at pressures of about  $10^{-5}$  Torr [53]. The wall plasma was initiated by having a voltage placed on a grid mounted inside the insulated channel. This plasma was found to be very homogeneous and stable in the pressure range of  $10^{-2}$  to  $10^{-5}$  Torr, and to be continuously controllable independently of the electron beam, which was passed through the center of the channel.

The insulated-wall plasma channel has a coaxial construction with the insulated channel inserted into a metal pipe and a grid cylinder placed on top of the insulator as shown in Fig. 31 [53]. Also shown in Fig. 31 is the experimental setup for the formation and diagnostic analysis of the wall plasma.

The plasma of the insulator wall was formed by applying a pulsed voltage on the grid electrode, thus forming a discharge between the grid electrode and the insulated channel surface. The mesh structure of the spark-initiating grid electrode allowed the discharge plasma to fill the volume of the channel.

The plasma was analyzed with the help of a double langmuir probe, a high ohmage voltage divider (D), an integrating Rogowski belt (RB),

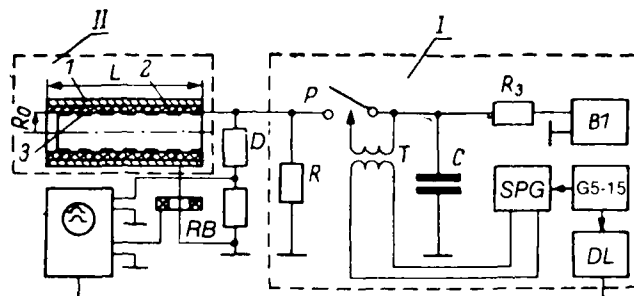


Fig. 31—Schematic diagram of experimental apparatus [53]

I—Voltage pulse generator

II—Plasma channel

1 —metal tube

2 —insulator channel

3 —grid electrode

P —discharge switch

B1 —high-voltage rectifier

SPG —spark pulse generator

G5-15 —pulse generator

DL —pulse delay line

D —high ohmage voltage divider

RB —Rogowski belt

photomultipliers, and a series of collectors. The experimental investigations demonstrated that in order to maintain a homogeneous wall plasma (characterized by an even distribution of the electron concentration  $N$ ), it is necessary to fulfill the following condition [53]:

$$W \geq (0.2 \text{ to } 0.6)S$$

where  $W$  = energy in the discharge circuit (in joules), and

$S$  = volume of the plasma channel ( $\text{cm}^3$ ).

With a  $W$  of less than  $0.2S$ , it was determined that the plasma possessed a multitongue structure and was inhomogeneous in  $N$ . The control of  $W$  was accomplished by varying the voltage on the capacitor  $C$  as well as its capacitance. The value of the electric field  $E$  between the grid electrode and the insulated channel wall was determined as a function of pressure (as shown in Fig. 32). This  $E$  determines the formation of the homogeneous plasma along the surface of the insulated wall as long as the condition described above is fulfilled.

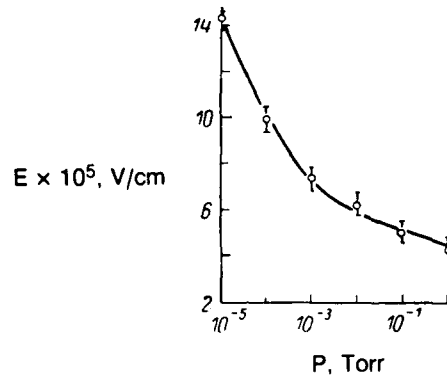


Fig. 32—Dependence of the electric field between the grid electrode and insulated channel wall upon the channel pressure [53]

The dependence of the electric field amplification coefficient  $K$  upon the metal grid wire diameter for different grid mesh sizes is shown in Fig. 33 [53].

From a series of measurements using a double langmuir probe and oscillograms, the distribution of the plasma electron concentration  $N$

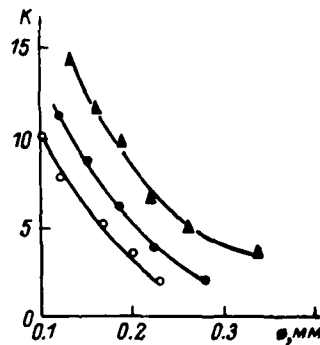


Fig. 33—Dependence of the electric field amplification coefficient  $K$  upon the metal grid wire diameter [53]

- — 2 × 2 mm grid mesh
- — 1.5 × 1.5 mm grid mesh
- ▲ — 1 × 1 mm grid mesh

was determined as a function of time  $T$  (in Fig. 34) and as a function of channel coordinates ( $R, L, \varphi$ ) (in Fig. 35) for a pressure of  $10^{-5}$  Torr in the channel, using a polyvinyl chloride plastic as the insulator wall material.

The dependence of  $N$  upon the pressure of the background gas  $P$  is shown in Fig. 36 [53].

From inspection of the above figures, one can see that the formation of the plasma is sufficiently homogeneous in the electron component concentration in the longitudinal as well as azimuthal directions. The weak dependence of  $N$  upon pressure demonstrates that the plasma is erosional in character, while the primary incomplete discharge along the insulator surface has a gas-discharge nature. The dispersion velocity of the plasma front was determined to be weakly dependent upon pressure and had a value of  $2$  to  $4 \times 10^6$  cm/s for most of the insulator wall materials.

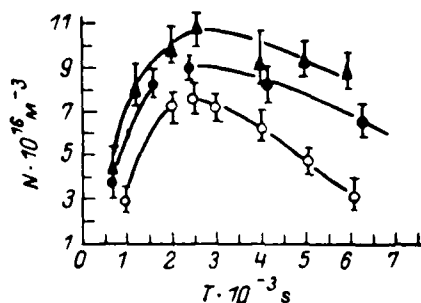


Fig. 34—Distribution of the plasma electron concentration  $N$  as a function of time  $T$  [53]

- —1,000 joules energy in the discharge circuit
- —1,600 joules energy in the discharge circuit
- ▲ —2,000 joules energy in the discharge circuit



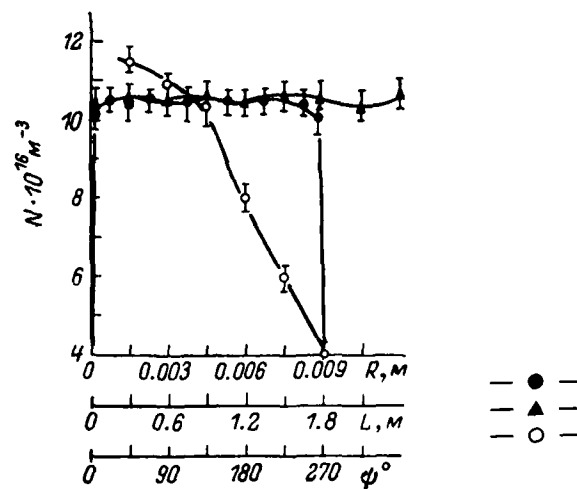


Fig. 35—Distribution of the plasma electron concentration  $N$  as a function of coordinates: length,  $L$ ; radius,  $R$ ; and azimuth,  $\varphi$ . Energy in the discharge circuit equal to 1,600 joules [53]

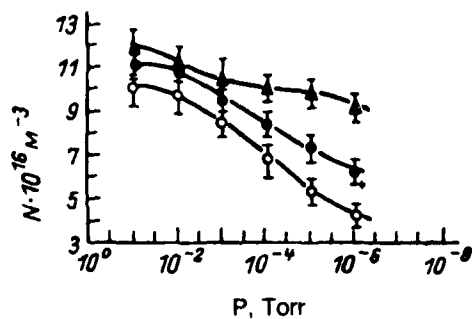


Fig. 36—Dependence of the plasma electron concentration component  $N$  as a function of the background gas  $P$  in a polyvinyl chloride insulator channel with energy in the discharge circuit of [53]:

- — 1,000 joules
- — 1,600 joules
- ▲ — 2,000 joules

#### IV. CONCLUSIONS

The available Soviet technical literature indicates an extensive Soviet interest in the transport of MeV, kA electron beams over long distances in air or other neutral gas. The effort level of Soviet research in this area, measured in terms of frequency of published papers, appears to have been increasing over the past five years. The published Soviet technical reports do not state the intended application of this research. An exception is the avowed interest, expressed in one theoretical paper, in transmitting high power for industrial purposes over distances on the order of 1000 km. Some theoretical and experimental work performed under laboratory conditions may have been aimed at solving beam transport problems within the inertial fusion program. However, some research, and especially that dealing with electron beam propagation in the ionosphere, may have military and space applications.

The main thrust of Soviet research in this area is the attempt to determine a gas-pressure "propagation window" that would optimize beam transport. The materials analyzed in this report show that Soviet researchers have considered all pressures from ultra-high-vacuum to atmospheric in this task, and appear to have singled out a narrow range of pressures that most of them agree to be optimal for IREB propagation:  $10^{-5} < P < 10^{-4}$  Torr. They find that at pressures below this propagation window the beam is no longer neutralized because of insufficient presence of positive ions in the beam. Above the transmission window, the beam transport efficiency drops because of background gas scattering and other effects.

There is a relatively large amount of recent Soviet research on IREB propagation through this pressure range and the related problem of propagation at ionospheric altitudes corresponding to these pressures. The Soviet theoretical and experimental approach to these problems also shows a great deal of ingenuity. The major theoretical effort was applied to obtain a quasi-equilibrium IREB, and to derive an analytical formula for its propagation through low-pressure gas, taking into account space charge forces, self-focusing of the beam, and the beam's own magnetic field. The objective was to obtain the most efficient propagation for a maximum beam current at long distances.

At low gas pressures, IREB transport depends, among other things, on an adequate supply of an ion space charge for effective beam neutralization. According to Soviet researchers, such a supply of ions can

be provided with the aid of insulated channels. By varying the length of the insulated channel, one can control the dispersion angle of the beam and the beam current density and its radial distribution. The Soviet development of a gridded insulated tube to obtain a cylindrical, homogeneous, stable, and continuously variable plasma in the pressure range from  $10^{-3}$  to  $10^{-5}$  Torr may be regarded as a model of the ion focusing mechanism that operates in low-pressure beam channels in gas. The insulated tube is claimed by the Soviets to be a good method of controlling plasma, making plasma independent of IREB parameters, and thus representing a new tool for IREB propagation.

## REFERENCES

AE	<i>Atomnaya energiya</i>
FM	<i>Fizicheskaya mekhanika</i>
FP	<i>Fizika plazmy</i>
Izv AN Armyanskoy SSR, Fizika	<i>Izvestiya Akademii nauk Armyanskoy SSR, seriya fizicheskaya</i>
PTE	<i>Pribory i tekhnika eksperimenta</i>
RiE	<i>Radiotekhnika i elektronika</i>
UFN	<i>Uspekhi fizicheskikh nauk</i>
UFZh	<i>Ukrainskiy fizicheskii zhurnal</i>
Vestnik LGU	<i>Vestnik Leningradskogo Universiteta</i>
ZhETF	<i>Zhurnal eksperimental'noy i teoreticheskoy fiziki</i>
ZhETF, Pis'ma	<i>Pis'ma v Zhurnal eksperimental'noy i teoreticheskoy fiziki</i>
ZhTF	<i>Zhurnal tekhnicheskoy fiziki</i>
ZhTF, Pis'ma	<i>Pis'ma v Zhurnal tekhnicheskoy fiziki</i>

1. Vlasov, M. A., S. I. Vybornov, A. V. Zharinov, S. V. Nikonov, "Propagation of an Intense Electron Beam in a Gas, Allowing for the Beam's Own Magnetic Field," *RiE*, Vol. 26, No. 3, 1981, p. 617.
2. Tosunyan, G. A., A. V. Zharinov, "Distribution of the Density of Plasma Formed by an Electron Beam in a Rarefied Gas," *RiE*, Vol. 26, No. 12, 1981, p. 2622.
3. Vlasov, M. A., S. V. Nikonov, "Non-collisional Relaxation of a Cold High-Current Electron Beam," *RiE*, Vol. 28, No. 5, 1983, p. 965.
4. Zaslavskiy, G. M., B. V. Chirikov, "Stochastic Instability of Non-linear Oscillations," *UFN*, Vol. 105, No. 1, 1971, p. 3.
5. Khodatayev, K. V., "A Feature of Propagation of an Electron Beam in Gas," *ZhETF, Pis'ma*, Vol. 18, No. 3, 1973, p. 184.
6. Meyerovich, B. Ye., S. T. Sukhoruchkov, "Equilibrium Structure of Relativistic Beams," *ZhETF*, Vol. 68, No. 5, 1975, p. 1783.

7. Vyalov, G. N., V. N. Yevteyev, Yu. M. Zolotaykin, K. N. Ul'yanov, "An Axially-Symmetric Electron Beam with Space Charge Neutralization," *ZhTF*, Vol. 44, No. 11, 1974, p. 2290.
8. Vlasov, M. A., Yu. A. Kovalenko, O. A. Malafeyev, S. V. Nikonov, "Magnetic Compression of a Relativistic Electron Beam," *RiE*, Vol. 26, No. 11, 1981, p. 2370.
9. Glebov, V. V., A. V. Zharinov, V. A. Malafayev, D. N. Novichkov, G. A. Tosunyan, "The Propagation Velocity of a Relativistic Electron Beam in a Rarefied Gas," *RiE*, Vol. 24, No. 8, 1979, p. 1594.
10. Glebov, V. V., D. N. Novichkov, "An Experimental Investigation of the Equilibrium of a Quasi-Neutral Relativistic Electron Beam in a Rarefied Gas," *RiE*, Vol. 28, No. 1, 1983, p. 143.
11. Glebov, V. V., A. V. Zharinov, V. V. Kantsel', D. N. Novichkov, K. V. Khodatayev, "Quasi-Equilibrium Processes of the Interaction of a Relativistic Electron Beam with a Rarefied Gas," *FP*, Vol. 1, No. 4, 1975, p. 662.
12. Glebov, V. V., V. A. Malafayev, D. N. Novichkov, "Measurement of the Integral Characteristics of Intense Pulsed Electron Beams," *PTE*, No. 2, 1979, p. 42.
13. Kovalenko, V. P., S. K. Pats'ora, "The Excitation of Ion Oscillations by a Freely-Propagating Electron Beam," *ZhETF*, Vol. 77, No. 3, 1979, p. 909.
14. Rosinskiy, S. Ye., A. A. Rukhadze, V. G. Rukhlin, "Mechanism of Ion Acceleration at the Gas Ionization Front by a Relativistic Electron Beam," *ZhETF, Pis'ma*, Vol. 14, No. 1, 1971, p. 53.
15. Tkach, Yu. V., I. I. Magda, G. V. Skachev, S. S. Pushkarev, I. P. Panchenko, "Transport of an Intense Relativistic Electron Beam Through Gas," *ZhTF*, Vol. 44, No. 3, 1974, p. 658.
16. Levine, L. S., I. M. Vitkovsky, D. A. Hammer, "Propagation of an Intense Relativistic Electron Beam Through a Plasma Background," *J. Appl. Phys.*, Vol. 42, 1971, p. 1863.
17. Rander, J., B. Ecker, G. Yonas, D. J. Drickey, "Charged-Particle Acceleration by Intense Electron Streams," *Phys. Rev. Lett.*, Vol. 24, 1970, p. 283.
18. Andrews, M., J. Bzura, H. H. Fleischmann, N. Rostoker, "Effects of a Magnetic Guide Field on the Propagation of Intense Relativistic Electron Beams," *Phys. Fluids*, Vol. 13, No. 5, 1970, p. 1322.
19. Zav'yalov, M. A., L. A. Luk'yanov, A. S. Murashov, V. I. Perevodchikov, L. P. Shanturin, M. P. Shemetov, "A 500 kV Electron Gun," *PTE*, No. 2, 1980, p. 223.
20. Zav'yalov, M. A., A. A. Kamunin, V. I. Perevodchikov, "Electrical-Optical Systems Based on a Spherical Diode with a Plasma Anode," *RiE*, Vol. 20, No. 7, 1975, p. 1466.

21. Guseva, G. I., M. A. Zav'yalov, "Development of Beam-Plasma Discharge During Transport of an Electron Beam in a Gas," *FP*, Vol. 9, No. 4, 1983, p. 770.
22. Didenko, A. N., V. S. Pak, Yu. P. Usov, V. I. Tsvetkov, A. A. Shatanov, N. S. Shulayev, "The Transport of an Intense Microsecond Electron Beam in a Neutral Gas," *ZhTF, Pis'ma*, Vol. 4, No. 7, 1978, p. 412.
23. Gleyzer, I. Z., V. S. Pak, Yu. P. Usov, V. I. Tsvetkov, A. A. Shatanov, "Propagation of High-Current Microsecond Beams in Vacuum Channels with Metal and Dielectric Walls," *ZhTF*, Vol. 50, No. 2, 1980, p. 396.
24. Didenko, A. N., Ye. T. Protasevich, V. V. Tikhomirov, "Transport of Intense Electron Beams Through Plasma Under Low Pressure," *ZhTF, Pis'ma*, Vol. 1, No. 15, 1975, p. 692.
25. Rudakov, L. I., V. P. Smirnov, A. M. Spektor, "The Behavior of an Intense Electron Beam in a Dense Gas," *ZhETF, Pis'ma*, Vol. 15, No. 9, 1972, p. 540.
26. Kolesnikov, Ye. K., A. P. Kuryshv, B. V. Filippov, "Parameters of Stabilized Electron Beams in the Upper Atmosphere," *Vestnik LGU*, No. 13, 1979, p. 84.
27. Kolesnikov, Ye. K., A. P. Kuryshv, B. V. Filippov, "Relativistic Electron Beam in the Upper Atmosphere," *FM*, No. 3, 1978, p. 78.
28. Rosinskiy, S. Ye., V. G. Rukhlin, "Dynamics of a Dense Electron Beam Injected into a Plasma," *ZhTF*, Vol. 42, No. 3, 1972, p. 511.
29. Dzhekson, D. Ye. [Jackson, D. J.], "NASA's Program for the Investigation of the Upper Atmosphere," in: *Elektronnaya kontsentratsiya v ionosfere i ekzosfere*, Moscow, 1966, p. 349-371.
30. Khaziakhmetova, T. Kh., A. P. Kuryshv, "Budker Instability of a Relativistic Electron Beam," *Vestnik LGU*, No. 19, 1980, p. 69.
31. Budker, G. I., "Relativistic Stabilized Electron Beam," *AE*, No. 5, 1956, p. 9.
32. Kuryshv, A. P., T. Kh. Khaziakhmetova, "Magnetic and Discharge Neutralization of a Relativistic Electron Beam Injected into a Highly-Magnetized Plasma," *FM*, No. 4, 1980, p. 211.
33. Kolesnikov, Ye. K., Yu. I. Meshcheryakov, B. V. Filippov, "Dynamics of the Initial Stage of the Spreading of a Dense High-Temperature Plasma," *FM*, No. 1, 1974, p. 92.
34. Gun'ko, Yu. F., A. V. Norin, "Large Spherical Probe in Weakly-Ionized Weakly-Nonstationary Plasma," *FM*, No. 4, 1980, p. 185.
35. Vavilov, S. A., Ye. K. Kolesnikov, "Dynamics of Highly-Charged Bodies in Space," *FM*, No. 4, 1980, p. 168.
36. Kolesnikov, Ye. K., A. P. Kuryshv, "Remote Spectroscopic Elemental Analysis of the Surface Rock of Heavenly Bodies Based on

- Characteristic Radiation Artificially Excited by Neutral Particle Beam," Vestnik LGU, No. 7, 1984, p. 130.
37. Gladkiy, A. M., V. P. Kovalenko, "Experimental Investigation of Quasi-Stationary Waves Excited During the Periodic Injection of Electron Bunches into a Plasma," ZhETF, Vol. 74, No. 3, 1978, p. 984.
  38. Kovalenko, V. P., "Electron Bunches in Nonlinear Collective Interaction of Beams with Plasma," UFN, Vol. 139, No. 2, 1983, p. 223.
  39. Kovalenko, V. P., "Excitation of Stationary Waves in a Plasma by the Injection of Cold Electron Bunches," FP, Vol. 5, No. 4, 1979, p. 804.
  40. Gladkiy, A. N., V. P. Kovalenko, "Phase Focusing of a Density-Modulated Electron Beam in Plasma," UFZh, Vol. 22, No. 8, 1977, p. 1246.
  41. Gabovich, M. D., V. P. Kovalenko, O. A. Metallov, O. K. Nazarenko, S. K. Pats'ora, "The Relative Role of Proper Electric and Magnetic Fields in Self-Focusing of Gas-Neutralized Electron Beams," ZhTF, Vol. 47, No. 7, 1977, p. 1569.
  42. Gabovich, M. D., V. P. Kovalenko, O. K. Nazarenko, S. K. Pats'ora, "A Possible Method of Neutralizing the Space Charge of Powerful Electron Beams Under Conditions of an Ultrahigh Vacuum," ZhTF, Pis'ma, Vol. 5, No. 10, 1979, p. 581.
  43. Kovalenko, V. P., V. M. Pergamenshchik, V. N. Starkov, "Quasi-Equilibrium States of a Pinching Electron Beam," ZhETF, Vol. 84, No. 6, 1983, p. 2055.
  44. Gabovich, M. D., V. P. Kovalenko, I. M. Mitropan, V. N. Starkov, S. F. Fastovets, "Combined Electron and Ion Beams—A Model of Evolving Collisionless Plasma," FP, Vol. 8, No. 4, 1982, p. 808.
  45. Krastelev, Ye. G., B. N. Yablokov, "Transport and Focusing of an Intense Electron Beam Through a Vacuum Chamber with Insulator Walls," ZhTF, Pis'ma, Vol. 3, No. 15, 1977, p. 775.
  46. Agafonov, A. V., A. Sh. Ayrapetov, A. A. Kolomenskiy, Ye. G. Krastelev, A. N. Lebedev, B. N. Yablokov, "Propagation and Focusing of an Intense Electron Beam in Dielectric Channels," FP, Vol. 7, No. 2, 1981, p. 267.
  47. Kazanskiy, L. N., A. A. Kolomenskiy, G. O. Meskhi, B. N. Yablokov, "High Current Electron Accelerator: Impul'se," AE, Vol. 42, No. 2, 1977, p. 113.
  48. Agafonov, A. V., A. Sh. Ayrapetov, A. A. Kolomenskiy, Ye. G. Krastelev, B. N. Yablokov, "Control of the High Current Beam Shape and Heavy Ion Beam Generation in Insulated Channels," Proceedings of the 4th International Topical Conference on High

- Power Electron and Ion Beam Research and Technology, Palaiseau, 1981, p. 715.
49. Akopov, R. A., O. G. Antablyan, Ye. K. Khanikyants, "The Effect of Insulated Channels on High-Current Relativistic Electron Beam Parameters," ZhTF, Vol. 53, No. 11, 1983, p. 2269.
  50. Akopov, R. A., O. G. Antablyan, Ye. K. Khanikyants, "Ribbon Relativistic Electron Beam in the Self-Focusing Regime," Izv AN Armyanskoy SSR, Fizika, Vol. 16, 1981, p. 397.
  51. Akopov, R. A., O. G. Antablyan, S. V. Davtyan, Ye. K. Khanikyants, "Optimization of Intensity and Energy Losses of an IREB during Transport through Neutral Gas," ZhTF, Vol. 54, No. 7, 1984, p. 1284.
  52. Akopov, R. A., O. G. Antablyan, Ye. K. Khanikyants, "Propagation of Intense Electron Beams through Curved Insulated Channels," Izv AN Armyanskoy SSR, Fizika, Vol. 16, No. 2, 1983, p. 121.
  53. Korenev, S. A., N. B. Rubin, "Formation of a Wall Plasma in Vacuum Drift Tubes," ZhTF, Vol. 53, No. 10, 1983, p. 1928.